R167G RNA-transfected cells (Fig. 7A and B, respectively) ($P < 0.05$ at 1, 10, 100, and 1,000 IU/ml), indicating that the MA/N3H+N5BX-JFH1/5am virus was more sensitive to interferon than the MA/JFH1.2/R167G virus, which contained more regions from JFH-1.

DISCUSSION

In this study, we developed a novel infectious HCV production system using a genotype 2b chimeric virus. To improve infectious virus production, we introduced two modifications into the chimeric genome.

First, we replaced the 5′ UTR from MA with that of JFH-1. Similarly to J6/JFH-1, replacement of the 5′ UTR increased core protein accumulation in both the cells and medium when these RNAs were transfected into Huh7.5.1 cells (Fig. 1). The same trend was observed when these RNAs were transfected into Huh7-25 cells (data not shown), indicating that the 5′ UTR of JFH-1 enhanced RNA replication. There are two genetic variations in J6CF and seven in MA in the region we replaced (nt 1 to 154 for J6CF and nt 1 to 155 for MA), and some of these mutations may affect RNA replication by changing the RNA secondary structure, RNA-RNA interactions, or binding of host or viral proteins.

Second, we introduced a cell culture-adaptive mutation (R167G) in the core region. This mutation was induced by long-term culture of MA/JFH-1 RNA-transfected cells (Fig. 2). MA/JFH-1 chimeric RNA (MA/JFH-1.1 and MA/JFH-1.2) replicated when synthesized RNA was transfected into the cells. However, infectious virus production was low, and virus infection did not spread over the short term. In early stages of long-term culture, the number of core protein-positive cells gradually decreased, and core protein-positive cells were scarcely detectable. Subsequently, the population of core protein-positive cells increased, reaching almost 100%. At this time point, we identified a common mutation in the core region (R167G) of the viral genome as a cell culture-adaptive mutation and found that it enhanced infectious virus production (Fig. 3). Several nonsynonymous mutations other than R167G were identified in the viral genome from each supernatant, and these mutations may enhance infectious virus production. However, there was a discrepancy between RNA levels and the infectivity of the culture media of MA/JFH-1.2 and MA/JFH-1.2/R167G RNA-transfected cells (Fig. 3C and D). The MA/JFH-1.2/R167G mutant had a 2-log increase in viral infectivity compared to that of MA/JFH-1.2 but only a 1-log increase in secreted RNA. The replication efficiency of MA/JFH-1.2 RNA-transfected cells was comparable to that of MA/JFH-1.2/R167G RNA-transfected cells, but the efficiency of infectious virus assembly within the cells was low, indicating that mainly noninfectious virus may be produced.

Infection of MA/JFH-1.2/R167G virus spreads rapidly, similarly to that of the JFH-1 virus, when it is inoculated into naïve Huh7.5.1 cells. On a single-cycle virus production assay, we found that the R167G mutation did not affect RNA replication or virus secretion but enhanced infectious virus assembly within the cells (Fig. 4). Efficient infectious virus assembly within the cells was mainly responsible for the rapid spread and high virus production of MA/JFH-1.2/R167G.

The amino acid at 167 (aa 167) is located in domain 2 of the core region, which is important for localization of the core protein (3, 8). Lipid droplet localization of the core protein and/or NS5A is important for infectious virus production (4, 18, 26). The interaction between the core protein and NS5A is also important for infectious virus production (16). Thus, aa 167 affects infectious virus production possibly by altering subcellular localization of the core protein or interaction between the core protein and NS5A. We examined the amino acid sequence of the core protein in 2,078 strains in the Hepatitis Virus Database (http://s2as02.genes.nig.ac.jp/) and found that aa 167 is Gly in all other strains. These data strongly suggest that Gly at aa 167 is important for the HCV life cycle. As the MA strain was cloned from the serum of a patient with chronic hepatitis C, the low virus production by this Gly at aa 167 may be important for persistent infection.

We then attempted to reduce the contents of JFH-1 from MA/JFH-1.2/R167G. We previously reported that the N3H and N5BX regions of JFH-1 were sufficient for replication of the J6CF strain (21). We also reported that this effect was observed only in genotype 2a strains (J6CF, JCH-1, and JCH-4). In this study, we tested whether the N3H and N5BX regions of JFH-1 could also support replication of a genotype 2b strain, MA. We constructed an MA chimeric virus harboring the N3H and N5BX regions of JFH-1 and combined this with the 5′ UTR of JFH-1 and the R167G mutation (MA/N3H+N5BX-JFH1/R167G). This chimeric RNA was able to replicate in the cells and produce infectious chimeric virus in culture medium although infectious virus production levels were low (Fig. 5).

We showed in this paper that the N3H and N5BX regions of JFH-1 were able to support RNA replication by both genotype 2a clones and genotype 2b clones, but the nucleotide sequence similarity between JFH-1 and MA was lower than that between JFH-1 and J6CF (77% versus 89%, respectively). Compared to MA/JFH-1.2/R167G, MA/N3H+N5BX-JFH1/R167G RNA showed the same levels of RNA replication and low levels of infectious virus production. To clarify whether there were any differences in the characteristics of the secreted virus, we performed density gradient ultracentrifugation with the MA/JFH-1.2/R167G and MA/N3H+N5BX-JFH1/R167G viruses. The distributions of the HCV core protein and infectivity showed similar profiles (data not shown).

The differences between MA/JFH-1.2/R167G and MA/N3H+N5BX-JFH1/R167G are the NS2, NS3 protease domain (N3P), and NS4A to NS5A regions. Nucleotide variation(s) other than aa 167 in these regions of the MA strain may be associated with reduced virus assembly. We identified four additional cell culture-adaptive mutations, L814S (NS2), R1012G (NS2), T1106A (NS3), and V1951A (NS4B), which resulted from long-term culture of MA/N3H+N5BX-JFH1/R167G RNA-transfected cells. Consequently, cells transfected with MA/N3H+N5BX-JFH1/5am constructed by insertion of these four adaptive mutations into MA/N3H+N5BX-JFH1/R167G replicated and produced infectious virus as efficiently as MA/JFH-1.2/R167G RNA-transfected cells (Fig. 6).

This system is able to contribute to studies into the development of antiviral strategies. It has been reported that HCV genotype 2a was more sensitive to interferon therapy than HCV genotype 2b in a clinical study (20). To assess the interferon resistance of genotype 2b, a cell culture system with multiple genotype 2b strains is necessary. The previously reported replicable genotype 2b chimeric virus harbored only structural

– 321 –

regions of 2b strains (6, 27). The 2b/JFH-1 chimeric virus containing the region of the core protein to NS2 from the J8 strain (genotype 2b) and the region of NS3 to 3′ X of JFH-1 was able to replicate and showed that there were no differences in interferon sensitivity among the JFH-1 chimeric viruses of other genotypes (6, 27). Another 2b/JFH-1 chimeric virus containing the regions of the core protein to NS2 (nt 342 to 2867) of a genotype 2b strain and of NS2 to 3′ UTR (nt 2868) of JFH-1 has been reported (6, 27). The authors reported that their 2b/JFH-1 chimeric virus was more sensitive to interferon than JFH-1 (6, 27). We developed the genotype 2b HCV cell culture system with another HCV genotype 2b strain (MA). We identified a virus assembly-enhancing mutation in the core region, the minimal JFH-1 regions necessary for replication, and four additional adaptive mutations that enhance infectious virus production and demonstrated that MA harboring the five adaptive mutations and the 5′ UTR and N3H and N5BX regions of JFH-1 (MA/N3H+N5BX-JFH1/5am) could replicate and produce infectious virus efficiently.

Using these novel genotype 2b chimeric viruses, we assessed interferon sensitivity. We found that MA/JFH-1.2/R167G chimeric virus and MA/N3H+N5BX-JFH1/5am virus were more sensitive to interferon than the JFH-1 virus (Fig. 7). Furthermore, we found that MA/N3H+N5BX-JFH1/5am was more sensitive to interferon than MA/JFH-1.2/R167G, indicating that the genetic variation(s) in the NS2, N3P, and NS4A to NS5A regions affect interferon sensitivity. Although genotype 2a viruses are more sensitive to interferon than genotype 2b viruses in clinical studies, JFH-1 displayed interferon resistance in our study.

These results suggest that the JFH-1 regions in the 2b/JFH-1 virus affect the interferon sensitivity of the chimeric virus. Moreover, it was reported that amino acid variations in E2, p7, NS2, and NS5A were associated with the response to peginterferon and ribavirin therapy in genotype 2b HCV infection (10). Therefore, our MA/JFH-1 chimeric virus harboring minimal regions from JFH-1 (MA/N3H+N5BX-JFH1/5am) is more suitable for assessing the characteristics of the MA strain than the MA/JFH-1 chimeric virus, which includes a nonstructural region from JFH-1 (MA/JFH-1.2/R167G). We showed here that replacement of the 5′ UTR and N3H and N5BX regions in MA with those from JFH-1 is able to convert MA into a replicable virus. Using the same strategy, numerous HCV cell culture systems with various genotype 2b strains, as well as genotype 2a strains, may be available.

In conclusion, we established a novel HCV genotype 2b cell culture system using a chimeric genome in MA harboring minimal regions from JFH-1. This cell culture system using the chimeric genotype 2b virus will be useful for characterization of genotype 2b viruses and the development of antiviral strategies.

REFERENCES

1. Akazawa D, et al. 2007. CD81 expression is important for the permissiveness of Huh7 cell clones for heterogeneous hepatitis C virus infection. J. Virol. 81:5036–5045.
2. Bartenschlager R, Lohmann V. 2000. Replication of hepatitis C virus. J. Gen. Virol. 81:1631–1648.
3. Boulant S, et al. 2006. Structural determinants that target the hepatitis C virus core protein to lipid droplets. J. Biol. Chem. 281:22236–22247.
4. Boulant S, Targett-Adams P, McLauchlan J. 2007. Disrupting the association of hepatitis C virus core protein with lipid droplets correlates with a loss in production of infectious virus. J. Gen. Virol. 88:2204–2213.
5. Choo QL, et al. 1989. Isolation of a cDNA clone derived from a blood-borne non-A, non-B viral hepatitis genome. Science 244:359–362.
6. Gottwein JM, et al. 2009. Development and characterization of hepatitis C virus genotype 1–7 cell culture systems: role of CD81 and scavenger receptor class B type I and effect of antiviral drugs. Hepatology 49:364–377.
7. Griffin S, et al. 2008. Genotype-dependent sensitivity of hepatitis C virus to inhibitors of the p7 ion channel. Hepatology 48:1779–1790.
8. Hope RG, McLauchlan J. 2000. Sequence motifs required for lipid droplet association and protein stability are unique to the hepatitis C virus core protein. J. Gen. Virol. 81:1913–1925.
9. Jensen TB, et al. 2008. Highly efficient JFH1-based cell-culture system for hepatitis C virus genotype 5a: failure of homologous neutralizing-antibody treatment to control infection. J. Infect. Dis. 198:1756–1765.
10. Kadokura M, et al. 2011. Analysis of the complete open reading frame of genotype 2b hepatitis C virus in association with the response to peginterferon and ribavirin therapy. PLoS One 6:e24514.
11. Kato T, et al. 2008. Hepatitis C virus JFH-1 strain infection in chimpanzees is associated with low pathogenicity and emergence of an adaptive mutation. Hepatology 48:732–740.
12. Kato T, et al. 2006. Cell culture and infection system for hepatitis C virus. Nat. Protoc. 1:2334–2339.
13. Kiyosawa K, et al. 1990. Interrelationship of blood transfusion, non-A, non-B hepatitis and hepatocellular carcinoma: analysis by detection of antibody to hepatitis C virus. Hepatology 12:671–675.
14. Lindenbach BD, et al. 2005. Complete replication of hepatitis C virus in cell culture. Science 309:623–626.
15. Lohmann V, et al. 1999. Replication of subgenomic hepatitis C virus RNAs in a hepatoma cell line. Science 285:110–113.
16. Masaki T, et al. 2008. Interaction of hepatitis C virus nonstructural protein 5A with core protein is critical for the production of infectious virus particles. J. Virol. 82:7964–7976.
17. Miyamoto M, Kato T, Date T, Mizokami M, Wakita T. 2006. Comparison between subgenomic replicons of hepatitis C virus genotypes 2a (JFH-1) and 1b (Con1 NK5.1). Intervirology 49:37–43.
18. Miyanari Y, et al. 2007. The lipid droplet is an important organelle for hepatitis C virus production. Nat. Cell Biol. 9:1089–1097.
19. Murakami K, Abe M, Kageyama T, Kamoshita N, Nomoto A. 2001. Down-regulation of translation driven by hepatitis C virus internal ribosomal entry site by the 3′ untranslated region of RNA. Arch. Virol. 146:729–741.
20. Murakami T, et al. 1999. Mutations in nonstructural protein 5A gene and response to interferon in hepatitis C virus genotype 2 infection. Hepatology 30:1045–1053.
21. Murayama A, et al. 2007. The NS3 helicase and NS5B-to-3′X regions are important for efficient hepatitis C virus strain JFH-1 replication in Huh7 cells. J. Virol. 81:8030–8040.
22. Murayama A, et al. 2010. RNA polymerase activity and specific RNA structure are required for efficient HCV replication in cultured cells. PLoS Pathog. 6:e1000885.
23. Pietschmann T, et al. 2006. Construction and characterization of infectious intragenotypic and intergenotypic hepatitis C virus chimeras. Proc. Natl. Acad. Sci. U. S. A. 103:7408–7413.
24. Pietschmann T, et al. 2009. Production of infectious genotype 1b virus particles in cell culture and impairment by replication enhancing mutations. PLoS Pathog. 5:e1000475.
25. Scheel TK, et al. 2008. Development of JFH1-based cell culture systems

– 322 –

for hepatitis C virus genotype 4a and evidence for cross-genotype neutralization. Proc. Natl. Acad. Sci. U. S. A. 105:997–1002.

26. Shavinskaya A, Boulant S, Penin F, McLauchlan J, Bartenschlager R. 2007. The lipid droplet binding domain of hepatitis C virus core protein is a major determinant for efficient virus assembly. J. Biol. Chem. 282: 37158–37169.

27. Suda G, et al. 2010. IL-6-mediated intersubgenotypic variation of interferon sensitivity in hepatitis C virus genotype 2a/2b chimeric clones. Virology 407:80–90.

28. Takeuchi T, et al. 1999. Real-time detection system for quantification of hepatitis C virus genome. Gastroenterology 116:636–642.

29. Wakita T, et al. 2005. Production of infectious hepatitis C virus in tissue culture from a cloned viral genome. Nat. Med. 11:791–796.

30. Yi M, Ma Y, Yates J, Lemon SM. 2007. Compensatory mutations in E1, p7, NS2, and NS3 enhance yields of cell culture-infectious intergenotypic chimeric hepatitis C virus. J. Virol. 81:629–638.

31. Yi M, Villanueva RA, Thomas DL, Wakita T, Lemon SM. 2006. Production of infectious genotype 1a hepatitis C virus (Hutchinson strain) in cultured human hepatoma cells. Proc. Natl. Acad. Sci. U. S. A. 103:2310–2315.

32. Zhong J, et al. 2005. Robust hepatitis C virus infection in vitro. Proc. Natl. Acad. Sci. U. S. A. 102:9294–9299.

– 323 –

Potent and selective inhibition of hepatitis C virus replication by novel phenanthridinone derivatives

Mohammed T.A. Salim [a], Hiroshi Aoyama [b,1], Kazuyuki Sugita [b], Kouichi Watashi [c], Takaji Wakita [c], Takayuki Hamasaki [a], Mika Okamoto [a], Yasuo Urata [d], Yuichi Hashimoto [b], Masanori Baba [a,*]

[a] Division of Antiviral Chemotherapy, Center for Chronic Viral Diseases, Graduate School of Medical and Dental Sciences, Kagoshima University, 8-35-1, Sakuragaoka, Kagoshima 890-8544, Japan
[b] Institute of Molecular and Cellular Biosciences, The University of Tokyo, Tokyo 113-0032, Japan
[c] Department of Virology II, National Institute of Infectious Diseases, Tokyo 162-8640, Japan
[d] Oncolys BioPharma Inc., Tokyo 105-0001, Japan

ARTICLE INFO

ABSTRACT

A number of novel phenanthridinone derivatives were examined for their inhibitory effect on hepatitis C virus (HCV) replication in Huh-7 cells harboring self-replicating subgenomic viral RNA replicons with a luciferase reporter (LucNeo#2). The activity of compounds was further confirmed by inhibition of viral RNA copy number in different subgenomic and full-genomic replicon cells using real-time reverse transcription polymerase chain reaction. Among the compounds, 4-butyl-11-(1,1,1,3,3,3-hexafluoro-2-hydroxypropan-2-yl)-7-methoxy-[1,3]dioxolo[4,5-c]phenanthridin-5(4H)-one (HA-719) was found to be the most active with a 50% effective concentration of $0.063 \pm 0.010\ \mu M$ in LucNeo#2 cells. The compound did not show apparent cytotoxicity to the host cells at concentrations up to 40 μM. Western blot analysis demonstrated that HA-719 reduced the levels of NS3 and NS5A proteins in a dose-dependent fashion in the replicon cells. Interestingly, the phenanthridinone derivatives including HA-719 were less potent inhibitors of JFH1 strain (genobtype 2a HCV) in cell-free virus infection assay. Although biochemical assays revealed that HA-719 proved not to inhibit NS3 protease or NS5B RNA polymerase activity at the concentrations capable of inhibiting viral replication, their molecular target (mechanism of inhibition) remains unknown. Considering the fact that most of the anti-HCV agents currently approved or under clinical trials are protease and polymerase inhibitors, the phenanthridinone derivatives are worth pursuing for their mechanism of action and potential as novel anti-HCV agents.

1. Introduction

Hepatitic C virus (HCV) infection is a worldwide problem. More than 130 million individuals are infected with this virus, and 3–4 million are newly infected every year. In general, HCV infection proceeds to chronic infection [1], which often induces liver cirrhosis and hepatocellular carcinoma [2] liver transplantation is the only way to rescue patients with the end-stage liver disorders caused by HCV infection [3]. Protective vaccines are not available so far, and pegylated interferon (PEG-IFN) and the nucleoside analog ribavirin are the standard treatment for HCV infection [4–6]. However, many patients cannot tolerate the serious side effects of PEG-IFN and ribavirin. Therefore, the development of novel agents with better efficacy and tolerability is still mandatory.

HCV is an enveloped virus belonging to the hepacivirus genus of the family *Flaviviridae* [7,8]. The viral genome consists of positive sense single RNA coding a polyprotein cleaved by viral and host proteases into four structural and six non-structural proteins. Non-structural proteins are involved in the replication of HCV genome [9]. The discovery of effective anti-HCV agents was greatly hampered by the lack of cell culture systems that allowed robust propagation of HCV in laboratories. However, the development of HCV RNA replicon systems [10] and recent success in propagating infectious virus particles in vitro have provided efficient tools for screening new antiviral agents against HCV replication [11,12]. Furthermore, replicons containing a reporter gene, such as luciferase and green fluorescence protein, have provided fast and reproducible screening of a large number of compounds for their antiviral activity [13–15].

Currently, two NS3 protease inhibitors, teraprevir and boceprevir, have been licensed and a considerable number of novel anti-HCV agents are under clinical trials [16,17]. Most of them are directly acting inhibitors of NS3 protease or NS5B polymerase. However, the

emergence of HCV mutants resistant to most of these agents has also been reported [18]. To circumvent the drug-resistance, it seems necessary to use more than two directly acting drugs targeting different molecules for inhibition of viral replication [19]. Thus, in addition to the protease and polymerase inhibitors, novel compounds with a unique mechanism of action are highly desired.

We have recently identified some compounds with a novel phenanthridinone structure as moderate inhibitors of HCV replication [20]. This prompted us to synthesize a number of phenanthridinone derivatives and investigate their anti-HCV activity. After optimization of chemical structures, we have obtained the compounds that exert anti-HCV activity in the nanomolar range. Interestingly, these compounds did not inhibit the enzymatic activity of NS3 protease or NS5B RNA polymerase at the concentrations capable of inhibiting HCV replication in replicon cells.

2. Materials and methods

2.1. Compounds

More than 100 phenanthridinone derivatives were synthesized and used in this study. The synthesis of these compounds has been described previously [20,21]. Cyclosporin A (CsA) was purchased from Sigma–Aldrish. All compounds were dissolved in dimethyl sulfoxide (DMSO) (Nacalai Tesque) at a concentration of 20 mM or higher to exclude the cytotoxicity of DMSO and stored at -20 °C until use.

2.2. Cells

Huh-7 cells were grown and cultured in Dulbecco's modified Eagle medium with high glucose (Gibco/BRL) supplemented with 10% heat-inactivated fetal bovine serum (Gibco/BRL), 100 U/ml penicillin G, and 100 µg/ml streptomycin. Huh-7 cells containing self-replicating subgenomic HCV replicons with a luciferase reporter, LucNeo#2 [22], were maintained in culture medium containing 1 mg/ml G418 (Nakarai Tesque). The subgenomic replicon cells without reporter #50-1 and the full-genomic replicon cells NNC#2 [23] were kindly provided by Dr. Hijikata (Kyoto University, Kyoto, Japan). These cells were also maintained in culture medium containing 1 mg/ml G418.

2.3. Anti-HCV assays

The anti-HCV activity of the test compounds was determined in LucNeo#2 cells by the previously described method with some modifications [24]. Briefly, the cells (5×10^3 cells/well) were cultured in a 96-well plate in the absence of G418 and in the presence of various concentrations of the compounds. After incubation at 37 °C for 3 days, the culture medium was removed, and the cells were washed twice with phosphate-buffered saline (PBS). Lysis buffer was added to each well, and the lysate was transferred to the corresponding well of a non-transparent 96-well plate. The luciferase activity was measured by addition of the luciferase reagent in a luciferase assay system kit (Promega) using a luminometer with automatic injectors (Berthold Technologies).

The activity of the test compounds was also determined by the inhibition of HCV RNA synthesis in LucNeo#2, #50–1, and NNC#2 cells [23,25]. The cells (5×10^3 cells/well) were cultured in a 96-well plate in the absence of G418 and in the presence of various concentrations of the compounds. After incubation at 37 °C for 3 days, the cells were washed with PBS, treated with lysis buffer in TaqMan® Gene Expression Cell-to-CT™ kit (Applied Biosystems), and the lysate was subjected to real-time reverse transcription polymerase chain reaction (RT-PCR), according to the

manufacturer's instructions. The 5'-untranslated region of HCV RNA was quantified using the sense primer 5'-CGGGAGAGCCA-TAGTGG-3', the antisense primer 5'-AGTACCACAAGGCCTTTCG-3', and the fluorescence probe 5'-CTGCGGAACCGGTGAGTACAC-3' (Applied Biosystems).

The inhibitory effect of the test compounds on the replication of a genotype 2a strain was evaluated by the infection of Huh-7.5.1 cells, kindly provided by Dr. Chisari at Scripps Institute, with cell-free JFH-1 virus, as previously described [11]. At 48 h after virus infection, the cells were treated with SideStep Lysis and Stabilization Buffer (Agilent Technologies), and the lysate was subjected to real-time RT-PCR for quantification of HCV RNA [25].

2.4. Cytotoxicity assay

Huh-7 cells (5×10^3 cells/well) were cultured in a 96-well plate in the presence of various concentrations of the test compounds. After incubation at 37 °C for 3 days, the number of viable cells was determined by a dye method using the water soluble tetrazolium Tetracolor One® (Seikagaku Corporation), according to the manufacturer's instructions. The cytotoxicity of the compounds was also evaluated by the inhibition of host cellular mRNA synthesis. The cells were treated with lysis buffer in the kit, as described above, and the cell lysate was subjected to real-time RT-PCR for amplification of a part of glyceraldehyde-3-phosphate dehydrogenase (GAPDH) RNA using a TaqMan® RNA control reagent (Applied Biosystems).

2.5. Immunoblotting

LucNeo#2 cells (5×10^3 cells/well) were cultured in a 96-well plate in the presence of various concentrations of the test compounds. After incubation at 37 °C for 4 days, the culture medium was removed, and the cells were washed with PBS and treated with lysis buffer (RIPA Buffer®, Funakoshi). The protein concentration of the lysate was measured by Bradford protein assay method (Bio-Rad). Then, the lysate was subjected to sodium dodecyl sulfate polyacrylamide gel electrophoresis (SDS–PAGE). The primary antibodies used for protein detection were anti-NS3 (Thermo Scientific), anti-NS5A (Acris Antibodies), and anti-GAPDH (Santa Cruz Biotechnology) mouse monoclonal antibodies.

2.6. Protease and polymerase inhibition assays

The effect of the test compounds on NS3 protease activity was determined by a fluorescence resonance energy transfer-based assay using SensoLyte® 520 HCV Assay Kit (AnaSpec), according to the manufacturer's instructions. The inhibition assay for NS5B polymerase was performed at 37 °C for 60 min in a 384-well plate. A reaction mixture (30 µl/well) contains 20 mM Tris–HCl (pH 7.6), 10 mM MgCl$_2$, 20 mM NaCl, 1 mM dithiothreitol, 0.05% Tween 20, 0.05% pluronic F127, 1 µM [^{3}H]GTP (0.1 µCi/well) plus cold GTP, 5 nM poly(rC), 62.5 nM biotinylated dG$_{12}$, 45 nM recombinant NS3 protease, and various concentrations of the compounds. The reaction was stopped by streatavidin scintillation proximity assay beads in 0.5 M ethylenediaminetetraacetic acid. The plate was counted with a microbeta reader on the following day.

3. Results

When a number of phenanthridinone derivatives were examined for their antiviral activity in LucNeo#2 cells, three phenanthridinone derivatives, 5-butyl-2-(1,1,1,3,3,3-hexafluoro-2-hydroxypropan-2-yl)-3,8-dimethoxyphenanthridin-6(5H)-one (KZ-16), 4-butyl-11-(1,1,1,3,3,3-hexafluoro-2-hydroxypropan-2-yl)-[1,3]dioxolo[4,5-c]

phenanthridin-5(4H)-one (HA-718), and 4-butyl-11-(1,1,1,3,3, 3-hexafluoro-2-hydroxypropan-2-yl)-[1,3]dioxolo[4,5-c]phenan-thridin-5(4H)-one (HA-718), and 4-butyl-11-(1,1,1,3,3,3-hexa-fluoro-2-hydroxypropan-2-yl)-7-methoxy-[1,3]dioxolo[4,5-c] phenanthridin-5(4H)-one (HA-719) (Fig. 1) proved to be highly potent and selective inhibitors of HCV (genotype 1b) replication. KZ-16, HA-718, and HA-719 reduced luciferase activity and viral RNA copy number in LucNeo#2 cells in a dose-dependent fashion (Fig. 2A–C). However, they did not affect the viability of Huh-7.5.1 cells at concentrations up to 40 μM (Fig. 2D). When the cytotoxicity of the compounds was evaluated by the copy number of GAPDH mRNA in the host cells, a similar result was obtained (data not shown).

Table 1 summarizes the anti-HCV activity of KZ-16, HA-718, and HA-719 in different (genotype 1b) replicon cells and in Huh-7 cells infected with cell-free JFH1 (genotype 2a) virus. The highest activity was achieved by HA-719 followed by KZ-16 and HA-718. The EC_{50} of KZ-16, HA-718, and HA-719 were 0.13 ± 0.04, 0.23 ± 0.06, and 0.063 ± 0.010 μM, respectively, in LucNeo#2 cells, when determined by the luciferase reporter activity. The 50% cytotoxic concentrations (CC_{50}) of all compounds were >40 μM. Therefore, the selectivity indices (SI), based on the ratio of CC_{50} to EC_{50}, of KZ-16, HA-718, and HA-719 were >307, >173, and >634, respectively. The anti-HCV activity of these compounds was confirmed by reduction of the viral RNA copy number in different replicon cells. However, they were less po-tent inhibitors of genotype 2a HCV (JFH1) replication in cell-free virus infection assay. Furthermore, the phenanthridinone deriva-tives were much less active in Huh-7 cells transfected with JFH1 rep-licons than in genotype 1b replicon cells (data not shown).

Immunoblot analysis was conducted to confirm that phenanth-ridinone derivatives were inhibitory to the expression of NS3 and NS5A proteins of HCV. As shown in Fig. 3, HA-719 strongly inhibited NS3 and NS5A expression in LucNeo#2 cells in a dose dependent fashion without affecting the expression of the host cellular protein GAPDH. The compound achieved 93% and 86% inhibition of NS3 and

NS5A, respectively, at a concentration of 0.5 μM, indicating that HA-719 is a potent inhibitor of HCV protein expression as well as viral RNA synthesis. Immunoblot analysis was also conducted for another phenanthridinone derivative, 2-(2-benzyloxy-1,1,1,3,3,3-hexafluoropropan-2-yl)-5-butyl-3-methoxyphenanthridin-6(5H)-one (KZ-37), of which anti-HCV activity was weaker than HA-719. KZ-37 also proved inhibitory to NS3 and NS5A expression in a dose-dependent fashion (data not shown).

In our attempt to elucidate the mechanism of action of the com-pounds, HA-719 was examined for their ability to inhibit the enzy-matic activity of genotype 1b NS3 protease and NS5B polymerase in cell-free assay systems. Little, if any, inhibition of NS3 protease activity was observed for HA-719. Its 50% inhibitory concentration (IC_{50}) for the protease was 5.7 μM (data not shown), which was much higher than its EC_{50} for HCV replication in replicon cells ($0.063–0.44$ μM). HA-719 did not show any inhibitory effect on NS5B polymerase activity at concentrations up to 20 μM (data not shown). Furthermore, KZ-37, of which EC_{50} for HCV replication was $2.1–4.8$ μM, was inactive against these two enzymes at a con-centration of 20 μM (data not shown). Thus, it is unlikely that the phenanthridinone derivatives suppress HCV replication by inhibit-ing the activity of either NS3 protease or NS5B polymerase.

4. Discussion

In this study, we have demonstrated that novel phenanthridi-none derivatives are potent and selective inhibitors of HCV replica-tion in vitro. Our previous study on the synthesis and antiviral activity of phenanthridinone derivatives demonstrated that some of them exhibited selective but moderate activity against HCV rep-lication in replicon cells [20,21]. After optimization of chemical structures, we succeeded in obtaining a series of potent and selec-tive derivatives (Fig. 1). Among them, the most active one was HA-719, a novel phenanthridinone derivative with a dioxole structure.

Previous studies of HCV replicon cell systems indicated that most replicons had cell culture-adaptive mutations, which arose during the selection process with G418 and enhanced replication efficiency [26–29]. Self-replicating subgenomic RNA replicons could be elimi-nated from Huh-7 cells by prolonged treatment with IFN, and a high-er frequency of cured cells could support the replication of subgenomic and full-genomic replicons [30]. The replication effi-ciency decreased with increasing amounts of transfected replicon RNA, indicating that viral RNA or proteins are cytopathic or that host cell factors in Huh-7 cells limit RNA amplification [31]. Therefore, both viral and cellular factors are considered to be important deter-minants for the efficiency of HCV replication in cell cultures, which may be able to explain the difference in EC_{50} values of the compounds among the subgenomic replicon cells used in this study (Table 1). Similarly, the difference in EC_{50} values in subgenomic and full-genomic replicon cells might be due to the difference of HCV RNA length or the difference of the host cells [32]. In fact, shorter RNA is known to replicate more efficiently than longer one [33].

The activity of phenanthridinone derivatives against the geno-type 2a strain JFH1 was weaker than that against genotype 1b (Ta-ble 1). Although the assay systems were not the same (replicon cell assay for genotype 1b versus cell-free virus infection assay for genotype 2b), the compounds were much less active against geno-type 2a (Table 1 and data not shown). Such difference in drug-sen-sitivity between genotype 1b and genotype 2a was previously reported and attributed to the genetic heterogeneity within the HCV genome [23]. In addition, the anti-HCV activity of compounds had been optimized in the genotype 1b replicon cells. HCV is clas-sified into 6 genotypes that are further separated into a series of subtypes [34,35]. Among the genotypes, genotype 1b virus is epi-demiologically predominant in Japan, and 65 and 17% of the cases
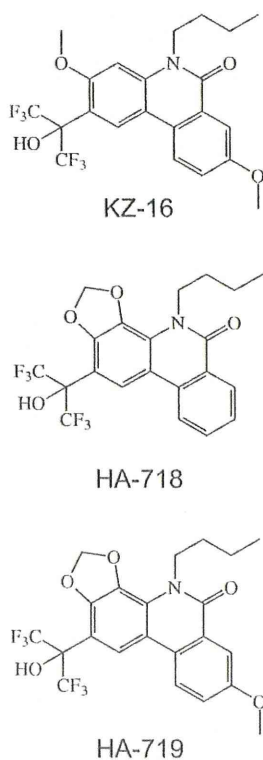

KZ-16

HA-718

HA-719

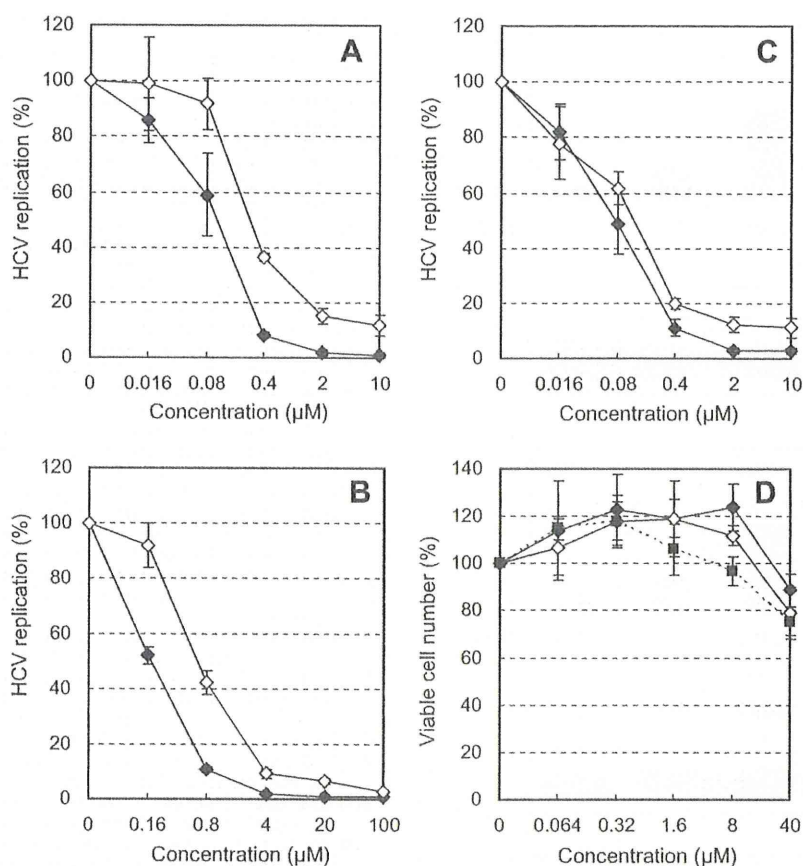**Fig. 1.** Chemical structures of phenanthridinone derivatives.

Fig. 2. Inhibitory effect of phenanthridinone derivatives on the replication HCV RNA replicons in LucNeo#2 cells and the proliferation of Huh-7 cells. LucNeo#2 cells were cultured in the presence of various concentrations of (A) KZ-16, (B) HA-718, or (C) HA-719. After incubation for 3 days, the cells were subjected to luciferase assay (closed diamond) and real-time RT-PCR (open diamond) to measure replicon-associated luciferase activity and RNA copy number, respectively, as parameters of HCV replication. (D) For the cell proliferation assay, Huh-7 cells were cultured in the presence of various concentrations of KZ-16 (closed diamond), HA-718 (open diamond), or HA-719 (closed square). After incubation for 3 days, the number of viable cells was determined by a tetrazolium dye method. Data represent means ± SD for triplicates experiments. Experiments were repeated at least twice, and a representative result is shown.

Table 1
Anti-HCV activity of phenanthridinone derivatives.

Compound		EC_{50} (μM)					CC_{50} (μM)
	Virus genotype	1b				2a	
	Cell	LucNeo#2		#50–1	NNC#2	Huh-7.5.1	Huh-7
	Assay	Luciferase	Real-time RT-PCR				Tetrazolium
KZ-16		0.13 ± 0.04	0.28 ± 0.01	0.40 ± 0.12	0.40 ± 0.14	2.6 ± 0.9	>40
HA-718		0.23 ± 0.06	0.68 ± 0.02	0.97 ± 0.56	0.90 ± 0.44	14 ± 5	>40
HA-719		0.063 ± 0.010	0.14 ± 0.01	0.25 ± 0.05	0.44 ± 0.20	4.9 ± 2.2	>40
CsA		0.24 ± 0.05	0.16 ± 0.01	0.18 ± 0.03	N.D.	0.58 ± 0.01	12 ± 3

EC_{50}: 50% effective concentration; CC_{50}: 50% cytotoxic concentration. N.D.: not determined.
Antiviral assay against the genotype 2a HCV was evaluated by the infection of Huh-7.5.1 cells with cell-free JFH-1 virus (see Section 2).
Except for the results in NNC#2 cells, all data represent means ± SD for three independent experiments. The data in NNC#2 cells represent means ± ranges for two independent experiments.

of HCV-related chronic hepatitis were caused by genotype 1b and genotype 2b, respectively [36].

At present, the target molecule of our phenanthridinone derivatives for inhibition of HCV replication remains unknown. Although it cannot be completely excluded that the compounds are inhibitors of NS3 protease or NS5B polymerase, biochemical assays revealed that HA-719 proved not to inhibit the activity of these enzymes at the concentrations capable of inhibiting viral replication. Therefore, the compounds may interact with another non-structural protein essential for viral replication, such as NS3

helicase and NS5A. In fact, a highly active inhibitor targeting NS5A has recently been identified [37]. Alternatively, the phenanthridinone derivatives may inhibit HCV replication through the interaction with host cellular factors deeply involved in HCV replication process [38–40]. It was reported that PJ34, a phenanthridinone derivative, had immunomodulatory activities and was protective against autoimmune diabetes [41], liver cancer [42], and stroke [43]. These studies suggested that the effects of PJ34 were attributed to the inhibition of poly(ADP-ribose) polymerase (PARP). Therefore, HA-719 was tested for its inhibitory effect on
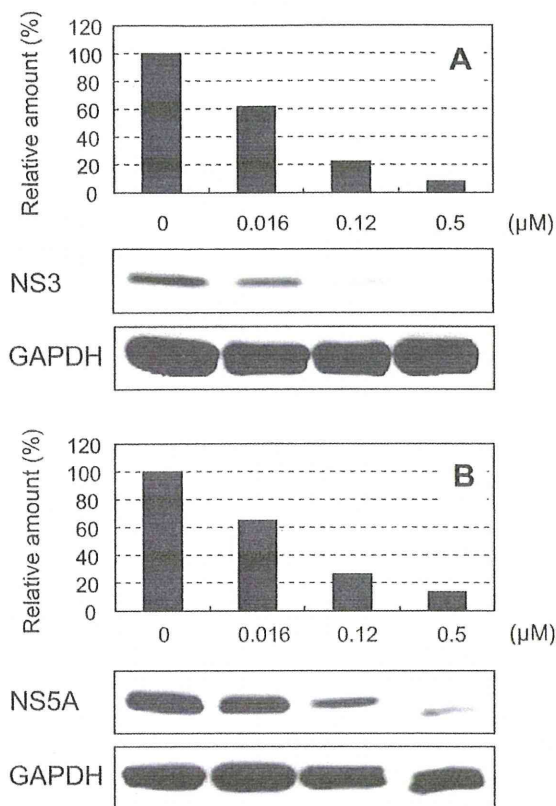
Fig. 3. Inhibitory effect of HA-719 on the expression of HCV proteins in LucNeo#2 cells. The cells were cultured in the presence of various concentrations of the compound. After incubation for 4 days, the cells were subjected to electrophoresis and immunoblot analysis for expression of (A) NS3 and (B) NS5A proteins. The band images were quantified by an image scanner and densitometer. Experiments were repeated at least twice, and a representative result is shown.

PARP activity and found to be inactive (data not shown). It was reported that some phenanthridinone derivatives had anti-human immunodeficiency virus (HIV) activity through the inhibition of viral integrase [44]. However, our compounds did not show selective inhibition of HIV replication in cell cultures (data not shown). Further studies, including the establishment of drug-resistant replicons, are in progress to determine the mechanism of action of the phenanthridinone derivatives.

In conclusion, our results clearly demonstrate that the novel phenanthridinone derivatives, especially HA-719, are highly potent and selective inhibitors of HCV replication in vitro. Although further studies, such as determination of their target molecule and pharmacological properties in vivo, are required, this class of compounds should be pursued for their clinical potential in the treatment of HCV infection.

Acknowledgments

References

[1] M. Koziel, M. Peters, Viral hepatitis in HIV infection, N. Engl. J. Med. 356 (2007) 1445–1454.

[2] J.H. Hoofnagle, Course and outcome of hepatitis C, Hepatology 36 (2002) S21–29.

[3] P. Sharma, A. Lok, Viral hepatitis and liver transplantation, Semin. Liver Dis. 26 (2006) 285–297.

[4] A.M. Di Bisceglie, J.H. Hoofnagle, Optimal therapy of hepatitis C, Hepatology 36 (2002) S121–127.

[5] M.W. Fried, M.L. Shiffman, K.R. Reddy, C. Smith, G. Marinos, F.L. Jr Gonçales, D. Häussinger, M. Diago, G. Carosi, D. Dhumeaux, A. Craxi, A. Lin, J. Hoffman, J. Yu, Peginterferon alfa-2a plus ribavirin for chronic hepatitis C virus infection, N. Engl. J. Med. 347 (2002) 975–982.

[6] A. Craxi, A. Licata, Clinical trial results of peginterferons in combination with ribavirin, Semin. Liver Dis. 23 (1) (2003) 35–46.

[7] Q.L. Choo, G. Kuo, A.J. Weiner, L.R. Overby, D.W. Bradley, M. Houghton, Isolation of a cDNA clone derived from a blood-borne non-A. Non-B viral hepatitis genome, Science 244 (1989) 359–362.

[8] M. Houghton, A. Weiner, J. Han, G. Kuo, Q.L. Choo, Molecular biology of the hepatitis C viruses: implications for diagnosis. Development and control of viral disease, Hepatology 14 (1991) 381–388.

[9] T. Suzuki, K. Ishii, H. Aizaki, T. Wakita, Hepatitis C viral life cycle, Adv. Drug Deliv. Rev. 59 (2007) 1200–1212.

[10] V. Lohmann, F. Korner, J.O. Koch, U. Herian, L. Theilmann, R. Bartenschlager, Replication of subgenomic hepatitis C virus RNAs in a hepatoma cell line, Science 285 (1999) 110–113.

[11] T. Wakita, T. Pietschmann, T. Kato, T. Date, M. Miyamoto, Z. Zhao, K. Murthy, A. Habermann, H.G. Krausslich, M. Mizokami, R. Bartenschlager, T.J. Liang, Production of infectious hepatitis C virus in tissue culture from a cloned viral genome, Nat. Med. 11 (2005) 791–796.

[12] M.B. Zeisel, T.F. Baumert, Production of infectious hepatitis C virus in tissue culture: a breakthrough for basic and applied research, J. Hepatol. 44 (2006) 436–439.

[13] R. Bartenschlager, The hepatitis C virus replicon system: from basic research to clinical application, J. Hepatol. 43 (2005) 210–216.

[14] R. Bartenschlager, Hepatitis C virus molecular clones: from cDNA to infectious virus particles in cell culture, Curr. Opin. Microbiol. 9 (2006) 416–422.

[15] V. Brass, D. Moradpour, H.E. Blum, Molecular virology of hepatitis C virus (HCV): 2006 update, Int. J. Med. Sci. 3 (2006) 29–34.

[16] L. Delang, L. Coelmont, J. Neyts, Antiviral therapy for hepatitis C virus: beyond the standard of care, Viruses 2 (2010) 826–866.

[17] C.M. Lange, C. Sarrazin, S. Zeuzem, Specifically targeted anti-viral therapy for hepatitis C – A new era in therapy, Aliment. Pharmacol. Ther. 32 (2010) 14–28.

[18] R.F. Schinazi, L. Bassit, C. Gavegnano, HCV drug discovery aimed at viral eradication, J. Viral Hepat. 17 (2010) 77–90.

[19] T.L. Kieffer, A.D. Kwong, G.R. Picchio, Viral resistance to specifically targeted antiviral therapies for hepatitis C (STAT-Cs), J. Antimicrob. Chemother. 65 (2010) 202–212.

[20] M. Nakamura, A. Aoyama, M.T.A. Salim, M. Okamoto, M. Baba, H. Miyachi, Y. Hashimoto, H. Aoyama, Structural development studies of anti-hepatitis C virus agents with a phenanthridinone skeleton, Bioorg. Med. Chem. 18 (2010) 2402–2411.

[21] H. Aoyama, K. Sugita, M. Nakamura, A. Aoyama, M.T.A. Salim, M. Okamoto, M. Baba, Y. Hashimoto, Fused heterocyclic amido compounds as anti-hepatitis C virus agents, Bioorg. Med. Chem. 19 (2011) 2675–2687.

[22] K. Goto, K. Watashi, T. Murata, T. Hishiki, M. Hijikata, K. Shimotohno, Evaluation of anti-hepatitis C virus effects of cyclophilin inhibitors, cyclosporine A, and NIM811, Biochem. Biophys. Res. Commun. 343 (2006) 879–884.

[23] N. Ishii, K. Watashi, T. Hishiki, K. Goto, D. Inoue, M. Hijikata, T. Wakita, N. Kato, K. Shimotohno, Diverse effects of cyclosporine on hepatitis C virus strain replication, J. Virol. 80 (2006) 4510–4520.

[24] M.P. Windisch, M. Frese, A. Kaul, M. Trippler, V. Lohmann, R. Bartenschlager, Dissecting the interferon-induced inhibition of hepatitis C virus replication by using a novel host cell line, J. Virol. 79 (2005) 13778–13793.

[25] K. Watashi, M. Hijikata, M. Hosaka, M. Yamaji, K. Shimotohno, Cyclosporine A suppresses replication of hepatitis C virus genome in cultured hepatocytes, Hepatology 38 (2003) 1282–1288.

[26] N. Appel, T. Pietschmann, R. Bartenschlager, Mutational analysis of hepatitis C virus nonstructural protein 5A: potential role of differential phosphorylation in RNA replication and identification of a genetically flexible domain, J. Virol. 79 (2005) 3187–3194.

[27] M. Ikeda, M. Yi, K. Li, S.M. Lemon, Selectable subgenomic and genome-length dicistronic RNAs derived from an infectious molecular clone of the HCV-N strain of hepatitis C virus replicate efficiently in cultured Huh7cells, J. Virol. 76 (2002) 2997–3006.

[28] M. Ikeda, K. Abe, H. Dansako, T. Nakamura, K. Naka, N. Kato, Efficient replication of a full-length hepatitis C virus genome, Strain O, in cell culture, and development of a luciferase reporter system, Biochem. Biophys. Res. Commun. 329 (2005) 1350–1359.

[29] M. Yi, S.M. Lemon, Adaptive mutations producing efficient replication of genotype 1a hepatitis C virus RNA in normal Huh7 cells, J. Virol. 78 (2004) 7904–7915.

[30] K.J. Blight, J.A. McKeating, C.M. Rice, Highly permissive cell lines for subgenomic and genomic hepatitis C virus RNA replication, J. Virol. 76 (2002) 13001–13014.

[31] V. Lohmann, S. Hoffmann, U. Herian, F. Penin, R. Bartenschlager, Viral and cellular determinants of hepatitis C virus RNA replication in cell culture, J. Virol. 77 (2003) 3007–3019.

[32] K. Abe, M. Ikeda, H. Dansako, K. Naka, N. Kato, Cell culture-adaptive NS3 mutations required for the robust replication of genome-length hepatitis C virus RNA, Virus Res. 125 (2007) 88–97.

[33] M. Rychlowska, K. Bieńkowska-Szewczyk, Hepatitis C – new developments in the studies of the viral life cycle, Acta Biochim. Pol. 54 (2007) 703–715.

[34] J. Bukh, R.H. Purcell, R.H. Miller, Sequence analysis of the core gene of 14 hepatitis C virus genotypes, Proc. Natl. Acad. Sci. USA 91 (1994) 8239–8243.

[35] O. Ohno, M. Mizokami, R.R. Wu, M.G. Saleh, K. Ohba, E. Orito, M. Mukaide, R. Williams, J.Y. Lau, New hepatitis C virus (HCV) genotyping system that allows for identification of HCV genotypes 1a, 1b, 2a, 2b, 3a, 3b, 4, 5a, and 6a, J. Clin. Microbiol. 35 (1997) 201–207.

[36] T. Kato, T. Date, M. Miyamoto, A. Furusaka, K. Tokushige, M. Mizokami, T. Wakita, Efficient replication of the genotype 2a hepatitis C virus subgenomic replicon, Gastroenterology 125 (2003) 1808–1817.

[37] M. Gao, R.E. Nettles, M. Belema, L.B. Snyder, V.N. Nguyen, R.A. Fridell, M.H. Serrano-Wu, D.R. Langley, J.H. Sun, D.R.I.I. O'Boyle, J.A. Lemm, C. Wang, J.O. Knipe, C. Chien, R.J. Colonno, D.M. Grasela, N.A. Meanwell, L.G. Hamann, Chemical genetics strategy identifies an HCV NS5A inhibitor with a potent clinical effect, Nature 465 (2010) 96–100.

[38] L. Coelmont, S. Kaptein, J. Paeshuyse, I. Vliegen, J.M. Dumont, G. Vuagniaux, J. Neyts, Debio 025, a cyclophilin binding molecule, is highly efficient in clearing hepatitis C virus (HCV) replicon-containing cells when used alone or in combination with specifically targeted antiviral therapy for HCV (STAT-C) inhibitors, Antimicrob. Agents. Chemother. 53 (2009) 967–976.

[39] P. Georgel, C. Schuster, M.B. Zeisel, F. Stoll-Keller, T. Berg, S. Bahram, T.F. Baumert, Virus-host interactions in hepatitis C virus infection: implications for molecular pathogenesis and antiviral strategies, Trends Mol. Med. 16 (2010) 277–286.

[40] T. Suzuki, A Hepatitis C virus-host interaction involved in viral replication: toward the identification of antiviral targets, Jpn. J. Infect. Dis. 63 (2010) 307–311.

[41] W.L. Suarez-Pinzon, J.G. Mabley, R. Power, C. Szabó, A. Rabinovitch, Poly (ADP-ribose) polymerase inhibition prevents spontaneous and recurrent autoimmune diabetes in NOD mice by inducing apoptosis of islet-infiltrating leukocytes, Diabetis 52 (2003) 1683–1688.

[42] S.H. Huang, M. Xiong, X.P. Chen, Z.Y. Xiao, Y.F. Zhao, Z.Y. Huang, PJ34, an inhibitor of PARP-1, Suppresses cell growth and enhances the suppressive effects of cisplatin in liver cancer cells, Oncol. Rep. 20 (2008) 567–572.

[43] G.E. Abdelkarim, K. Gertz, C. Harms, J. Katchanov, U. Dirnagl, C. Szabó, M. Endres, Protective effects of PJ34, a novel, potent inhibitor of poly(ADP-ribose) polymerase (PARP) in vitro and in vivo models of stroke, Int. J. Mol. Med. 7 (2001) 255–260.

[44] S. Patil, S. Kamath, T. Sanchez, N. Neamati, R.F. Schinazi, J.K. Buolamwini, Synthesis and biological evaluation of novel 5(H)-phenanthridin-6-ones, 5(H)-phenanthridin-6-one diketo acid, and polycyclic aromatic diketo acid analogs as new HIV-1 integrase inhibitors, Bioorg. Med. Chem. 15 (2007) 1212–1228.

PLoS one

Genetic Variation of the *IL-28B* Promoter Affecting Gene Expression

Masaya Sugiyama[1,2,5], Yasuhito Tanaka[3], Takaji Wakita[4], Makoto Nakanishi[2], Masashi Mizokami[1]*

1 The Research Center for Hepatitis and Immunology, National Center for Global Health and Medicine, Ichikawa, Chiba, Japan, 2 Department of Biochemistry and Cell Biology, Nagoya City University Graduate School of Medical Sciences, Mizuho, Nagoya, Japan, 3 Department of Virology and Liver Unit, Nagoya City University Graduate School of Medical Sciences, Mizuho, Nagoya, Japan, 4 Department of Virology II, National Institute of Infectious Diseases, Shinjuku, Tokyo, Japan, 5 JSPS Research Fellow, Japan Society for the Promotion of Science, Chiyoda, Tokyo, Japan

Abstract

The current standard of care for the treatment of chronic hepatitis C is pegylated interferon-α (PEG-IFNα) and ribavirin (RBV). The treatment achieves a sustained viral clearance in only approximately 50% of patients. Recent whole genome association studies revealed that single nucleotide polymorphisms (SNPs) around *IL-28B* have been associated with response to the standard therapy and could predict treatment responses at approximately 80%. However, it is not clear which SNP is most informative because the genomic region containing significant SNPs shows strong linkage disequilibrium. We focused on SNPs in close proximity to the *IL-28B* gene to evaluate the function of each and identify the SNP affecting the *IL-28B* expression level most. The structures of *IL-28A/B* from 5' to 3'-UTR were determined by complete cDNA cloning. Both *IL-28A* and *28B* genes consisted of 6 exons, differing from the CCDS data of NCBI. Two intron SNPs and a nonsynonymous SNP did not affect *IL-28B* gene function and expression levels but a SNP located in the proximal promoter region influenced gene expression. A (TA) dinucleotide repeat, rs72258881, located in the promoter region was discovered by our functional studies of the proximal SNPs upstream of *IL-28B*; the transcriptional activity of the promoter increased gradually in a $(TA)_n$ length-dependent manner following IFN-α and lipopolysaccharide stimulation. Healthy Japanese donors exhibited a broad range of (TA) dinucleotide repeat numbers from 10 to 18 and the most prevalent genotype was 12/12 (75%), differing from the database (13/13). However, genetic variation of *IL-28A* corresponding to that of *IL-28B* was not detected in these Japanese donors. These findings suggest that the dinucleotide repeat could be associated with the transcriptional activity of *IL-28B* as well as being a marker to improve the prediction of the response to interferon-based hepatitis C virus treatment.

Introduction

A novel group of cytokines was discovered simultaneously by two independent groups in 2003 and named interferon lambda (IFN-λ) [1,2] or type III IFN. Type III IFN comprises three members, IFN-λ1, 2, and 3 or *IL-29* and *IL-28A*, and *IL-28B*, respectively. Type III IFN is a member of the class II cytokine family. This family includes type I, II, and III interferons and the IL-10 family (IL-10, IL-19, IL20, IL-22, IL-24, and IL-26). IFN-λ uses a distinct receptor complex consisting of a unique subunit, named IFN-λR1, and the IL-10R2 subunit. Expression of the IFN-λR1 receptor subunit is highly restricted, whereas the type I IFN receptor complex and the IL-10R2 receptor were detected in most cell types [1,2,3,4,5,6]. The IL-10R2 receptor subunit is shared by IL-10, IL-22, IL-24, IL-26, and IFN-λ. This suggests that type III IFNs act in a rather cell-type specific manner to mediate their biological functions. Type III IFNs trigger a type I IFN-like gene expression profile [5,6,7], which has been shown to have antiviral activity *in vitro* and *in vivo* [1,2,5,6,8]. Thus, the two types of IFN seem to have similar biological effects at a cellular level. IFN-α and IL-29/28A treatment reduced the concentration

of hepatitis C virus (HCV) plus-strand RNA in an *in vitro* assay [6,9,10,11]. In addition, IL-29 may have therapeutic value against chronic viral hepatitis in human patients [5].

Recently, a genome-wide association study (GWAS) revealed that several highly correlated common single nucleotide polymorphisms (SNPs), in a linkage disequilibrium (LD) block encompassing the *IL-28B* genes on chromosome 19q13, are implicated in the response of chronic hepatitis C (CHC) patients to pegylated IFN-alpha (PEG-IFNα) and ribavirin (RBV) [12,13,14]. The CC genotype of rs12979860 and TT genotype of rs8099917 are associated in CHC patients with a sustained viral response (SVR) of 2.5 or greater rate, which is dependent of ethnicity, compared to the other genotypes. Moreover, the CC genotype of rs12979860 and TT genotype of rs8099917 favor spontaneous clearance of HCV [15].

We have reported the genomic analysis of approximately 15 kb containing the significant SNPs using Haploview software for LD and haplotype structure [14,16]. To analyze the difference in LD pattern between races, we performed LD mapping with these SNPs on JPT (Japanese in Tokyo), CEU (Utah residents with ancestry from Northern and Western Europe) or YRI (Yoruba in

– 330 –

Ibada, Nigeria) populations. These SNPs were in strong LD in JPT and CEU populations, although relatively low LD was predicted in the YRI population [14,16], suggesting that any of the SNPs located in this region could be responsible for treatment response. Because of the strong LD, tests for independence among these variants were not able to reveal which of these SNPs is uniquely responsible for the association with virological response (VR) or non-virological response (NVR). The identification of the primary genetic variant located in the LD block remained critical, although the risk haplotype tended to influence the expression levels or activity of IL-28B [13,14]. In this study, we sought to determine the primary SNP affecting IL-28B expression and/or its function by focusing on the proximal regulatory region of IL-28B.

IL-28B was discovered as a member of the IFN-λ family by Sheppard et al. and Kotenko et al. [1,2]. They discovered this family, IL-29, IL-28A, and IL-28B and the specific receptor, IL-28R1, by applying individual computational techniques to the draft human genome. However, the start codon of IFN-λ differs between the reports, with an additional 12 nucleotides at the N-terminus in all IFN-λs reported by Sheppard et al. (Fig. S1). The sequence similarity between these ORFs is approximately 96.7% and, especially, there is a high degree of identity between IL-28A and IL-28B cDNA (approximately 98%). Figure 1A shows the locations of IL-28A/B gene, the significant SNPs around IL-28B related to anti-HCV therapy reported in previous studies [12,13,14], and (TA)$_n$ repeats in the regulatory region of IL-28A and B. The SNPs information assessed in this study is summarized in Table 1 and the locations of the SNPs are shown in the schematic of the IL-28B gene (Fig. 1B). The reference sequences of IL-28A or IL-28B cDNA, registered in NCBI CCDS, are composed of 6 exons and 5 exons, respectively (Fig. 1B). Because high sequence similarity was observed between IL-28A and IL-28B from CpG to the region downstream of 3'-UTR (Fig. S2), the genes were almost completely identical around transcription start

site (TSS) (>99%). Then, we determined the likely gene structure using a complete cDNA cloning method because a similar transcriptional mechanism was expected for IL-28A and IL-28B.

Materials and Methods

Genome samples

Genome samples were obtained from 20 healthy volunteers (HV). Peripheral blood mononuclear cells (PBMC) collected from HV were isolated using the BD Vacutainer CPT Method (BD Biosciences). Genomic DNAs were extracted by standard methods. SNPs were selected from the database at GWAS database (https://gwas.lifesciencedb.jp/cgi-bin/gwasdb/gwas_top.cgi). Written informed consent was provided by all participants in the genotyping study following procedures approved by the Ethical Committee at Nagoya City University.

Cell lines

Human hepatocellular carcinoma cell lines, HepG2 and HuH7, human hepatocyte cell lines, HuSE2 (kindly provided by Dr. Hijikata in Kyoto University), and the human cervical cancer cell line, HeLa (obtained from The American Type Culture Collection), were cultured in Dulbecco's modified Eagle's medium supplemented with 10% (v/v) fetal bovine serum, 100 U ml^{-1} penicillin and 100 mg ml^{-1} streptomycin. Human leukemia virus type 1 transformed cell line, MT-2 (a gift from Dr. Ueda in Nagoya City University), Burkitt lymphoma cell line, Raji, and human T cell leukemia cell line, Jurkat (obtained from The American Type Culture Collection), were cultured in RPMI 1640 medium supplemented with 10% (v/v) fetal bovine serum, 100 U ml^{-1} penicillin and 100 mg ml^{-1} streptomycin. All incubations were performed at 37°C in a 5% CO$_2$ gassed incubator. Recombinant human IFN-λ2 and -3 were purchased from R&D Systems (Abingdon, UK). Natural human IFN-α was
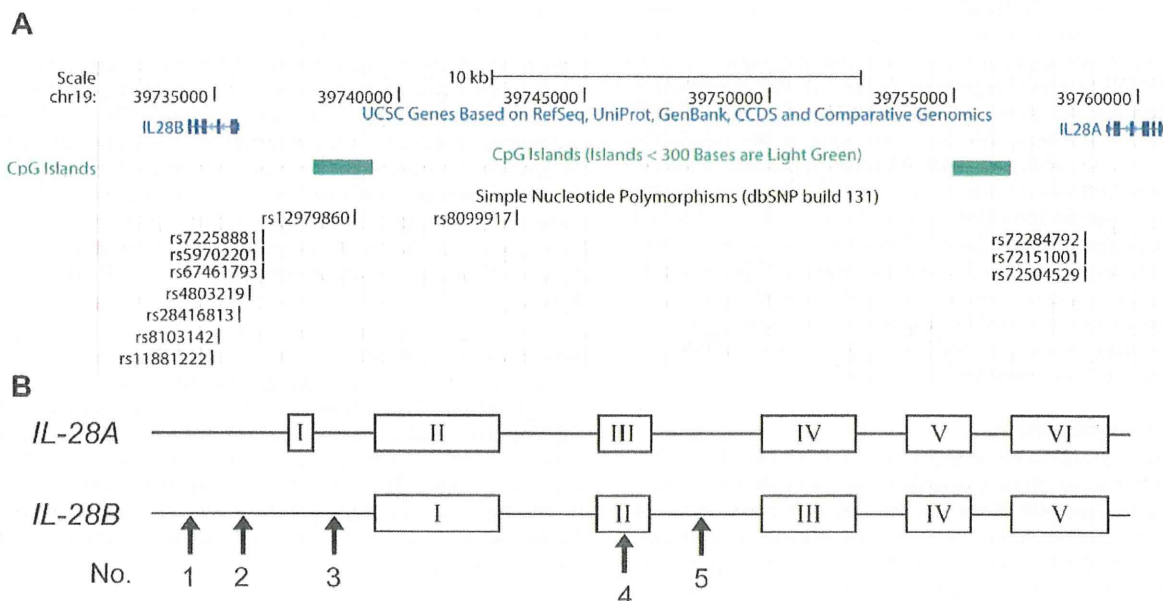
Figure 1. The position of significant SNPs and IL-28A/B in chromosome 19, retrieved from the database. (A) The IL-28A/B genes located in chromosome 19q13 are described in the genome map of the UCSC genome browser. The significant proximal SNPs around IL-28B associated with response to PEG-IFN/RBV therapy are shown in the map [14]. SNPs of (TA)$_n$ variation at the regulatory region of IL-28A are displayed in the position corresponding to that of IL-28B, which is not associated with anti-HCV therapy. (B) The schematic of IL-28A/B gene structure is described based NCBI CCDS data. Arrows show five significant SNPs examined in this study (see Table 1).
doi:10.1371/journal.pone.0026620.g001

– 331 –

Table 1. Significant SNPs around *IL-28B*.

Feature	rs ID	Allele 1/2[*1]	Minus strand[*2]	Location	No.
DIP[*3]	rs72258881[*4]	ATAT/-	TATA/-	Regulatory	1
Substitution	rs4803219	C/T	G/A	Regulatory	2
	rs28416813	C/G	G/C	Intron	3
	rs8103142	T/C	A/G	Nonsynonymous	4
	rs11881222	A/G	T/C	Intron	5

[*1]These data were derived from dbSNP. Allele 2 is the risk allele of HCV therapy reported by Tanaka et al., except for rs72258881.
[*2]Complementary nucleotides are shown because *IL-28B* is coded on the minus strand.
[*3]DIP: deletion/insertion polymorphism.
[*4]The ID represents rs72258881, rs59702201, and rs67461793 because these three are located in the same genomic region, the TA repeat.
doi:10.1371/journal.pone.0026620.t001

purchased from Hayashibara co. ltd. (Okayama, Japan). The mRNA expression levels of receptors stimulated in this study were confirmed by PCR using gene specific primer (Table S1 and Fig. S3),

Plasmid Construction

As a T/G heterozygote genome of rs8099917 with a strong LD was used as the PCR template, amplicons from the major and minor alleles were obtained for the assay described below. PCR was carried out to amplify the fragment from −858 nt of the ATG site to TGA of *IL-28B*, and the products were inserted into pcDNA3.1/Hyg (pcDNA/MA or mi) or pcDNA3.1/Hyg vector deleting CMV promoter (pdCMV/MA or mi). A FLAG sequence was conjugated to 6th exon, removing the stop codon, for real time PCR analysis. The promoter region from nucleotide position −858 to +30 of *IL-28B* was amplified using pdCMV/MA or mi vector and inserted into pGL4 vector for the luciferase assay. A vector with an antisense insert was prepared as a control. For expression constructs, the wild type (WT) plasmids, pcDNA3.1/wild expressing human IL-28B, and pcDNA3.1/ns-mut expressing human IL-28B harboring a K[74]R mutation, were generated using pcDNA3.1/V5-His-TOPO® (Invitrogen, San Diego, CA) and were used in the subsequent transfections. In addition, pcDNA3.1/AS expressing antisense strand of IL-28B was constructed as a control. We also obtained a pISRE-luc plasmid (provided by Sakamoto N., Tokyo Medical Dental University, Tokyo, Japan). The pGL4.74 vector encoding Renilla Luciferase was purchased from Promega (Madison, WI). These primer sequences are available on request. The above expression vectors were modified for the analysis of splicing function by introducing two intron SNPs (rs28416813 and rs11881222) (Table 1), which were pcDNA/WT, d-iSNPs.

Transient transfections

Transient transfections of HeLa, Jurkat, Raji, HuH7, HepG2, or HuSE2 (hepatocellular carcinomas cell line) cells were carried out using FuGene HD (Roche) or the Cell Line Nucleofector kit (Amaxa Biosystems) according to the manufacturers' protocols. Briefly, Cells (2×10^5) were seeded into a 6 well plate and transfected with for FuGene HD. For the electroporation method, cells (1.0×10^6) were collected and resuspended in Nucleofector solution V for each individual transfection sample.

5′-, 3′-RACE based on full-length cDNA cloning

Total RNA was prepared from cell lines stimulated with lipopolysaccharide (LPS) (0127:B8, Sigma-Aldrich) for 4 hours

after 100 U/mL of IFN-α for 16 hours by following previous paper [17]. A GeneRacer Kit (Invitrogen Life Technologies) was used to obtain the complete cDNA sequence of *IL-28A/B* following manufacturer's instructions. Briefly, the GeneRacer RNA Oligo was ligated to the 5′ end specifically of full-length mRNA within the total RNA mixture. This ligated mRNA was then converted to cDNA using reverse transcriptase (RT) and the GeneRacer Oligo dT Primer. Next, this cDNA was used for PCR using the oligonucleotides of GeneRacer 5′ Primer and P1 primer which hybridized to the coding strand of the *IL28A/B* (Table S1). The resulting PCR products were then used for a second round of PCR using the oligonucleotides GeneRacer 5′ Nested Primer, which represents the DNA equivalent of the 3′ end of the GeneRacer RNA Oligo, and P2, which hybridizes to the coding strand of the *IL-28A/B* 5′ to the P1 hybridization site. For 3′ RACE, the cDNA was subjected to the polymerase chain reaction (PCR) to amplify the 3′ end using a forward gene-specific primer P3 designed from *IL-28A/B* and the GeneRacer 3′ primer provided with the kit. Nested PCR, using the same gene-specific primer and GeneRacer 3′ nested primer, was performed. The PCR product of 5′ and 3′ RACE was cloned into pCR4-TOPO TA vector according to the manufacturer's instructions (Invitrogen). Ten clones were isolated and subjected to automated sequencing (ABI3100, ABI) in our core facility.

Protein expression and purification

Recombinant IL-28B and its mutant were produced by transfecting Free-Style™ 293-F cells (purchased from Invitrogen, Carlsbad, CA) with the expression plasmid, which was grown in 5000 ml of FreeStyle 293 Expression Medium, following the manufacturer's recommendations (Invitrogen, Carlsbad, CA). Cultures were maintained at >90% viability on a shaker plate (Titer Plate Shaker; Lab-Line Instruments, Melrose Park, NJ) moving at 125 rpm in a 37°C incubator with 8% CO_2 and subculturing at a 1:10 ratio upon reaching a density of 2×10^6 cells per ml. Cell density and viability were evaluated with a hemocytometer using 0.4% trypan blue staining. After 96 h, the transfected cell culture was harvested. The supernatant containing the secreted recombinant protein was centrifuged (100×g, 15 min), frozen, and stored at −30°C until use. The 293-F cells supernatant containing the recombinant protein was loaded onto a Ni^{2+} column (Amersham Biosciences) following the manufacturer's directions. Fractions were eluted with 80, 100, 250, and 1000 mM imidazole (in 50 mM Tris, 300 mM NaCl, pH 8.0), and the fraction eluted at 250 mM was pooled and concentrated in an Amicon (10 kDa molecular weight cutoff) to 1 ml (Amersham Biosciences).

Western blot analyses

Purified recombinant protein was loaded onto 12% sodium dodecyl sulfate gels. Proteins were detected with goat anti-IL28 (1:2000) polyclonal antibody (Santa Cruz Biotechnology, Santa Cruz, CA) and the secondary antibody. Proteins were visualized using ECL Plus Western blotting detection reagents (GE Healthcare) and a LuminoImager (LAS-3000; Fujifilm). The band densities were analyzed with the Multi Gauge software (version 3.1; Fujifilm).

IL-28A/B promoter genotyping

Germ-line DNA was extracted from PBMC according to standard methods [14]. Twenty HV samples were genotyped for the dinucleotide insertion/deletion (indel) present in the promoter region of *IL-28A* or *B*, as described below. Twenty ng of genomic DNA were subjected to PCR analysis in 50 μl aliquots containing

– 332 –

– 333 –

Figure 2. The determination of *IL-28B* gene structure and UTR region. *IL-28A/B* cDNA was isolated using a complete cDNA cloning method and the entire sequences were determined using HeLa, MT-2, and Raji call lines and PBMC from healthy volunteers. (A) 5'- and 3'-RACE analyses were used to determine the complete sequence of *IL-28A/B* mRNA after LPS stimulation (3 μg/mL) for 4 h following IFN-α treatment (100 U/mL) for 16 h. A representative example of agarose gel electrophoresis is shown for the non-stimulated control (NC). PCR products were inserted into the cloning vector and 6 clones of 5'- and 3'-RACE were analyzed by sequencing. (B) mRNA sequences of the 5' terminal region were aligned using CCDS retrieved from NCBI and RACE data of *IL-28A/B*. The upper two sequences are reference sequences from the NCBI CCDS and the lower two are representative sequences of *IL-28A* and *28B* obtained from 5'-RACE. The underlined triplet indicates the start codon of each gene and arrow shows the splice junctions. (C) mRNA sequences of the 3' terminal region were aligned using CCDS retrieved from NCBI and RACE data from *IL-28A/B*. The double-underlined triplet indicates the stop codon of each gene and arrows show the splice junctions. The polyA signal and representative site of polyadenylation also are shown. (D) The derived gene structure of the *IL-28B* is shown with the significant SNPs. The location of SNP No. 3 was changed from the regulatory to an intron region. The transcription start site (TSS) is found behind SNP No. 2.
doi:10.1371/journal.pone.0026620.g002

20 pmol of each primer, 5×PrimeSTAR GXL Buffer, 2.5 mM each deoxynucleotide triphosphates, and 1.25 units of PrimeStar GXL DNA polymerase (TAKARA Bio Inc, Tokyo, Japan). The primer pair, G1 and G2 (listed in Table S1), was used for the simultaneous amplification of the *IL-28A* and *28B* regulatory regions. The PCR conditions were as follows: 30 cycles of 10 s at 98°C, and 120 s at 68°C in addition of initial denaturation at 98°C for 5 min and a final extension at 68°C for 10 min. To separate the *IL-28A* amplicon from that of *IL-28B*, 10 μl of PCR products were analyzed using agarose gel electrophoresis and extracted with QIAquick Gel Extraction Kit (Qiagen). Each extracted product was analyzed by direct sequencing using Seq1 and Seq2 primers (Table S1). For further testing of the TA repeat, heterozygous samples were cloned into the pGEM-Teasy vector to count the number of TA repeats in each allele. Six clones were isolated and subjected to sequencing analysis using the primers described above.

Reporter assay

Luciferase assays of recombinant protein were performed using Dual-Glo Luciferase reporter assay system (Promega, Fitchburg, WI). In toll-like receptor (TLR)-stimulated experiments Raji cells were transfected and left for 16 h with 100 U/mL of IFN-α, then were exposed to LPS (3 μg/ml) for 4 h before harvesting. For assessments of recombinant protein, HeLa cells were transfected with pISRE-Luc and pGL4.74, and were harvested 24 h after IFN-α or λ treatment. The chemiluminescence was measured by SpectraMax L (Molecular Devices, Sunnyvale, CA). Firefly luciferase activity was normalized to Renilla activity to adjust for transfection efficiency.

Real-time PCR detection

Jurkat cells were transfected with the *IL-28B* expression vector harboring a FLAG sequence derived from the natural promoter (pdCMV/MA, mi, or AS). To induce IL-28B expression, TLR and IFN-α stimulation was given as described above. FLAG and glyceraldehyde-3-phosphate dehydrogenase (GAPDH) mRNA expression were measured using a real-time PCR performed on ABI Prism 7700 sequence detection system (Applied Biosystems) using primer sets (Table S1) after total RNA extraction and reverse transcription (RT) using an RT kit and TaqMan Universal PCR master mix (both Applied Biosystems), according to the manufacturer's manual. Relative gene expression was calculated as a fold induction compared to the control. Data were analyzed by the 2[-Delta Delta C(t)] method using Sequence Detector version 1.7 software (Applied Biosystems) [18] and were normalized using human GAPDH. A standard curve was prepared by serial 10-fold dilutions of human cDNA or FLAG plasmid. The curve was linear over 7 logs with a 0.998 correlation coefficient.

Statistical Analysis

Statistical analyses were conducted by using SPSS software package (SPSS 18J, SPSS, Chicago, IL) and Microsoft Excel 2007

(Microsoft co., Redmond, WA). Discrete variables were evaluated by Fisher's exact probability test. The P values were calculated by two-tailed student's t-tests for continuous data and chi-square test for categorical data, and those of less than 0.05 were considered as statistically significant.

Results

The identification of IL-28B gene structure

To define the human *IL-28A* or *IL-28B* gene structure, 5'-RACE and 3'-RACE were performed on total extracted RNA from HeLa, MT-2, Raji, HuH7 cells, and PBMCs from healthy volunteers (Fig. 2A). The sequences obtained matched the genomic contig of AC011445, which contains the sequence of *IL-28A* and *IL-28B* in forward and reverse orientations, respectively. All intron/exon junctions conformed to the canonical GT-AG rule. After stimulation of cells with LPS (3 μg/ml) for 4 h following IFN-α treatment (100 U/mL) for 16 h, *IL-28A/B* transcripts were detected in RACE experiments, but these were not detected in unstimulated cells. The representative TSSs are shown in Fig. 2B and showed little variation among cloned mRNA transcripts. The same 3'-UTR fragment also was detected without any intron in the 3'-RACE experiments (Fig. 2C). A polyadenylation signal (AAAUAAA), located in the 3'-UTR, was found upstream of the polyadenylation site in all samples. All sequences from the transcripts were aligned on the 5'-UTR, the six exons, and the 3'-UTR region of *IL-28A/B*. No different mRNA transcripts of *IL-28A/B* were found in our experiment. Taken together, the *IL-28B* gene structure comprised six exons (see Fig. 2D), and the location of SNP no. 3 (rs28416813) is in an intron, rather than a regulatory region (Table 1).

The effect of regulatory SNPs on promoter activity

Because the TSS was upstream of the position described in previous reports (Fig. 2), two rSNPs (rs72258881 and rs4803219) in the regulatory region were more specifically located in the TSS. A luciferase reporter approach was used to assess the effects of the two rSNPs on promoter activity. Luciferase vectors harboring the rSNPs were constructed and used for transfections (Fig. 3A). The promoter activities of the constructs were measured after stimulation with LPS (3 μg/ml) for 4 h following IFN-α treatment (100 U/mL) for 16 h. The transcriptional activity of constructions harboring the (TA)₁₁ mutation was reduced (Fig. 3B). Substitution in the rSNP (rs4803219) showed little effect on the transcriptional activity, whereas the number of TA repeats could be responsible for the putative region controlling basal transcription. To confirm the transcriptional activity, Jurkat cells were transfected with full length constructs expressing the FLAG sequence under the control of the natural promoter (Fig. 3C). To avoid the detection of endogenous mRNA, the mRNA with the FLAG sequence was specifically detected by real time PCR using the FLAG primer. The constructs harboring (TA)₁₁ yielded lower expression levels
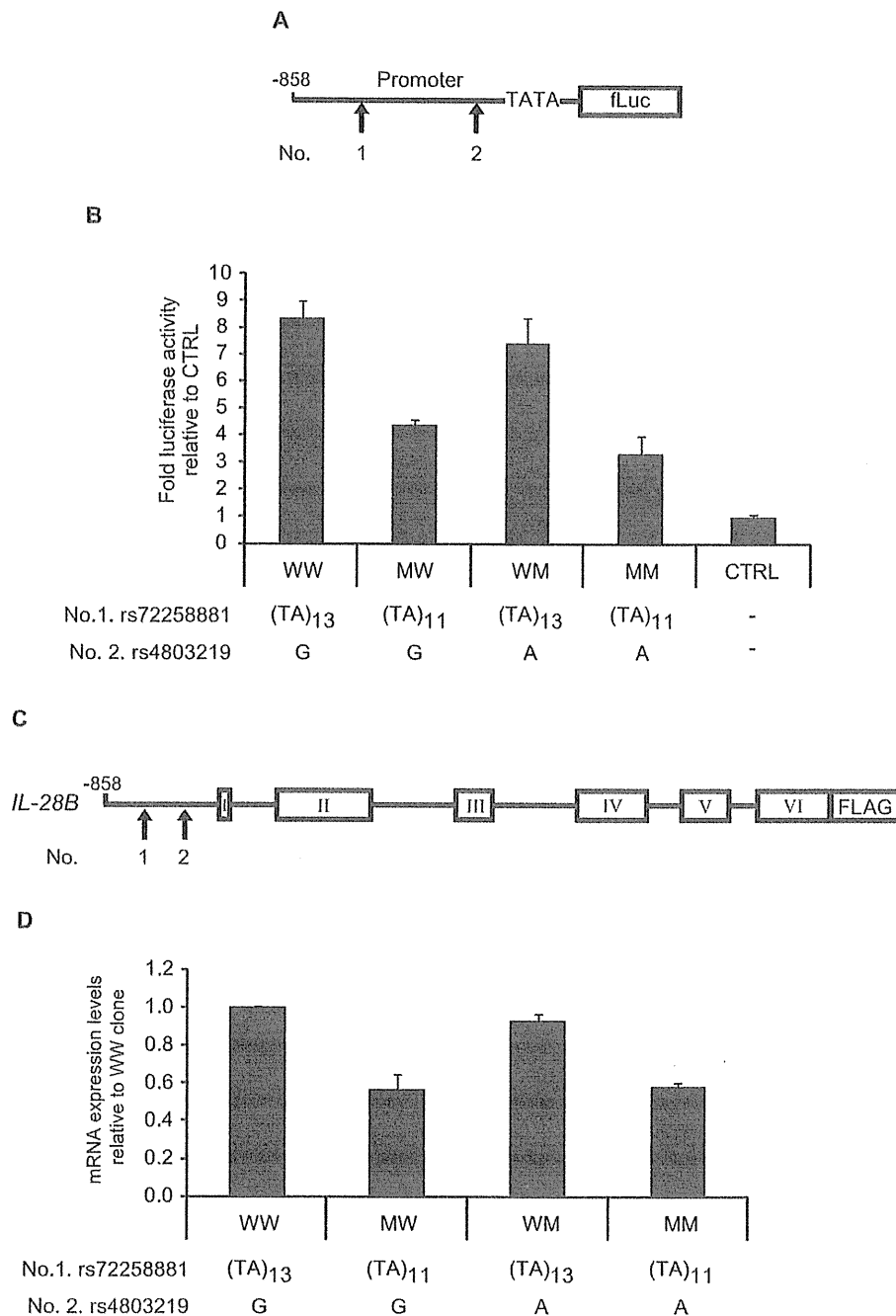
– 334 –

Figure 3. Transcriptional activity of the *IL-28B* promoter region compared between major and minor alleles. (A) The pGL4 reporter plasmid was constructed by subcloning the *IL-28B* promoter subfragment (nt −858 to +30). The combinations of two regulatory SNPs (rs72258881 or rs4803219) were introduced into the pGL4 vector (pGL4/WW, MW, WM, and MM). (B) Raji cells were co-transfected with pGL4 plasmids (0.05 g), and pGL4.74 control plasmid (0.05 g), and tested for firefly as well as renilla luciferase after LPS stimulation (3 μg/mL) for 4 h following IFN-α treatment (100 U/mL) for 16 h. These cells were seeded in a 96-well plate at 10^4 cells/well. The luciferase activities were normalized with renilla activities and data are presented as fold induction from activation of control vector. Bars indicate the means ± SD of triplicate determinations and the results are from one of three experiments. Statistical analyses are shown in table S2 to avoid complication. (C) For real-time PCR, the combinations of two regulatory SNPs (rs72258881 or rs4803219) were introduced into the pdCMV vector harboring a FLAG sequence (pdCMV/WW, MW, WM, and MM). (D) Jurkat cells were co-transfected with pdCMV plasmids (0.05 μg) and secreted alkaline phosphatase (SEAP) control plasmid (0.05 μg) and the expression levels were quantified using specific primer after LPS and IFN-α stimulation. The FLAG expression levels were normalized with SEAP activities and GAPDH as described in method section. Data are presented as fold induction from expression levels of pdCMV/WW. Bars indicate the means ± SD of triplicate determinations and the results are from one of three experiments. Statistical analyses are shown in table S3 to avoid complication.

doi:10.1371/journal.pone.0026620.g003

- 335 -

after IFN-α and LPS stimulation (Fig. 3D), suggesting that the length of TA repeat in the regulatory region of *IL-28B* could affect the regulation of *IL-28B* transcription.

Two intron SNPs located near the branch site of splicing

To determine the effect of the two iSNPs on pre-mRNA splicing, HeLa cells were transfected with wild type (WT), a construct with a double mutation of the iSNPs (d-iSNPs), or an antisense (AS) plasmid driven by the CMV promoter (Fig. 4A). The construct providing antisense transcription controlled by the CMV promoter was used to control for splicing defects (AS). Transcripts were analyzed by RT-PCR using primers in exon 1–2, 3–4, and 4–5. The RNA isolated from the WT and d-iSNPs yielded a single band using the three primer pairs. In contrast, longer amplicons were generated in cells expressing the antisense construct (Fig. 4B). The PCR products were sequenced to confirm the origin of the aberrant splicing events derived from the antisense construct (data not shown). The sequence analyses confirmed that PCR products from the WT and d-iSNPs were generated by normal splicing, suggesting that these two intron SNPs resulted in no splicing defects under these conditions.

No effect of nonsynonymous SNPs on IL-28B function

A nonsynonymous SNPs (rs8103142) located in the 3rd exon (Table 1 and Fig. 2D) led to the amino acid substitution $K^{74}R$ (Fig. 5A). Interestingly, the amino acid at this position is almost always arginine in homologous mammalian IFN-λs (e.g. human IL-28A, mouse IL-28A/B, and rhesus IL-28A/B). Then, the $K^{74}R$ substitution was expected to change IL-28B activity. The purified recombinant IL-28B protein (wild type) and the variant (ns-mut) were recognized by anti-IL-28B polyclonal antibody in a western blot assay (Fig. 5B). Based on spectrophotometric measurement of the protein concentration of the eluted fraction, it was calculated that at least 360 μg/mL of purified recombinant IL-28B protein (wild type and ns-mut) was obtained after purification. Flow-through liquid without recombinant protein was provided in the column preparing the sample of pcDNA3.1/AS (Fig. 5B). Molecular processing of IL-28B protein was confirmed to

determine the precise N-terminal amino acid by peptide sequencer as the processing site of signal peptide was predicted by computer simulation (http://www.uniprot.org/uniprot/Q8IZI9). Then, the N-terminal sequence, VPVAR, was obtained (data not shown), suggesting that the simulation data was consistent with the form of physiological protein.

To evaluate the effect of nsSNPs on ISRE activity, three hepatoma cell lines (HuH7, HepG2, and HuSE2) expressing IL-28R1 and IL-10R2 were transfected with pISRE-Luc and pGL4.74. These recombinant proteins were added to the supernatant (5 ng/mL each). As shown in Fig. 5C, ISRE activity of the ns-mut protein was similar to that of wild type protein in each cell line. IFN-α (100 U/mL), as a positive control of ISRE activity, showed a strong ISRE activity. These results suggested that the nonsynonymous mutation of rs8103142 did not affect IL-28B activity *in vitro*.

The genetic variation of TA repeats at the upstream of *IL-28B*

The reference sequence (RefSeq) of the human genome in the international database registers the TA repeat SNPs, rs72284729 or rs72258881, in the regulatory regions of *IL-28A* and *IL-28B*, respectively. The registered basal number of $(TA)_n$ is 8 in the regulatory region of *IL-28A* on the plus strand, whereas that of *IL-28B* is 13 on the minus strand encoding the gene (Table 2). From 20 Japanese healthy volunteers, genomic DNA was extracted to determine the actual $(TA)_n$ number located in the region of *IL-28A* or *IL-28B* by direct sequencing and, when direct sequencing chromatographs of $(TA)_n$ heterozygotes showed mixed patterns from the end of the TA repeat (Fig. S4), the mixed samples were subjected to cloning analysis. Interestingly, the $(TA)_n$ number in *IL-28A* was consistently different from dbSNP data, whereas that of *IL-28B* showed varying numbers along with SNPs data. The $(TA)_n$ range of *IL-28B* was from 10 to 18, and the most prevalent genotype was 12/12 (75%) in healthy Japanese volunteers.

To determine the functional significance of the TA indel, the regulatory region from −858 bp to +30 bp modifying the $(TA)_n$ number was cloned into the pGL4 reporter vector, transfected into HeLa cells, and assessed for firefly luciferase reporter gene
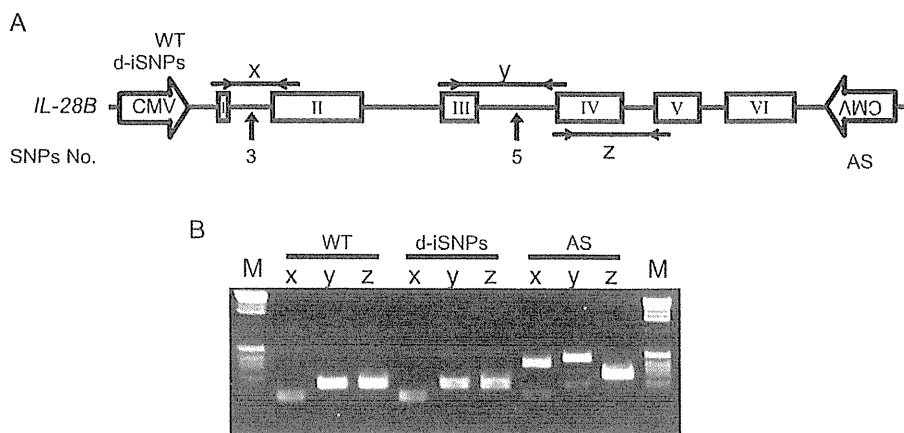
A

B

Figure 4. The determination of intron SNPs located near the branch site of splicing. (A) The expression plasmid of WT, d-iSNPs, or antisense (AS) derived from the CMV promoter was transfected into HeLa cells. Schematic of the WT, d-iSNPs, or AS used in the transfection experiments. PCR primers were designed to amplify products between exons. The effect of No. 3 and 5 SNPs (rs28416813 or rs11881222) on splicing were examined by amplicons x and y, respectively. The amplicon z was used for a splicing control. (B) Isolated RNAs were amplified by RT-PCR. The amplified products were checked by 2% agarose gel electrophoresis. The bands from the AS plasmid transcribing antisense represented abnormal splicing of mRNA as a control. Results shown are representative of three independent experiments.
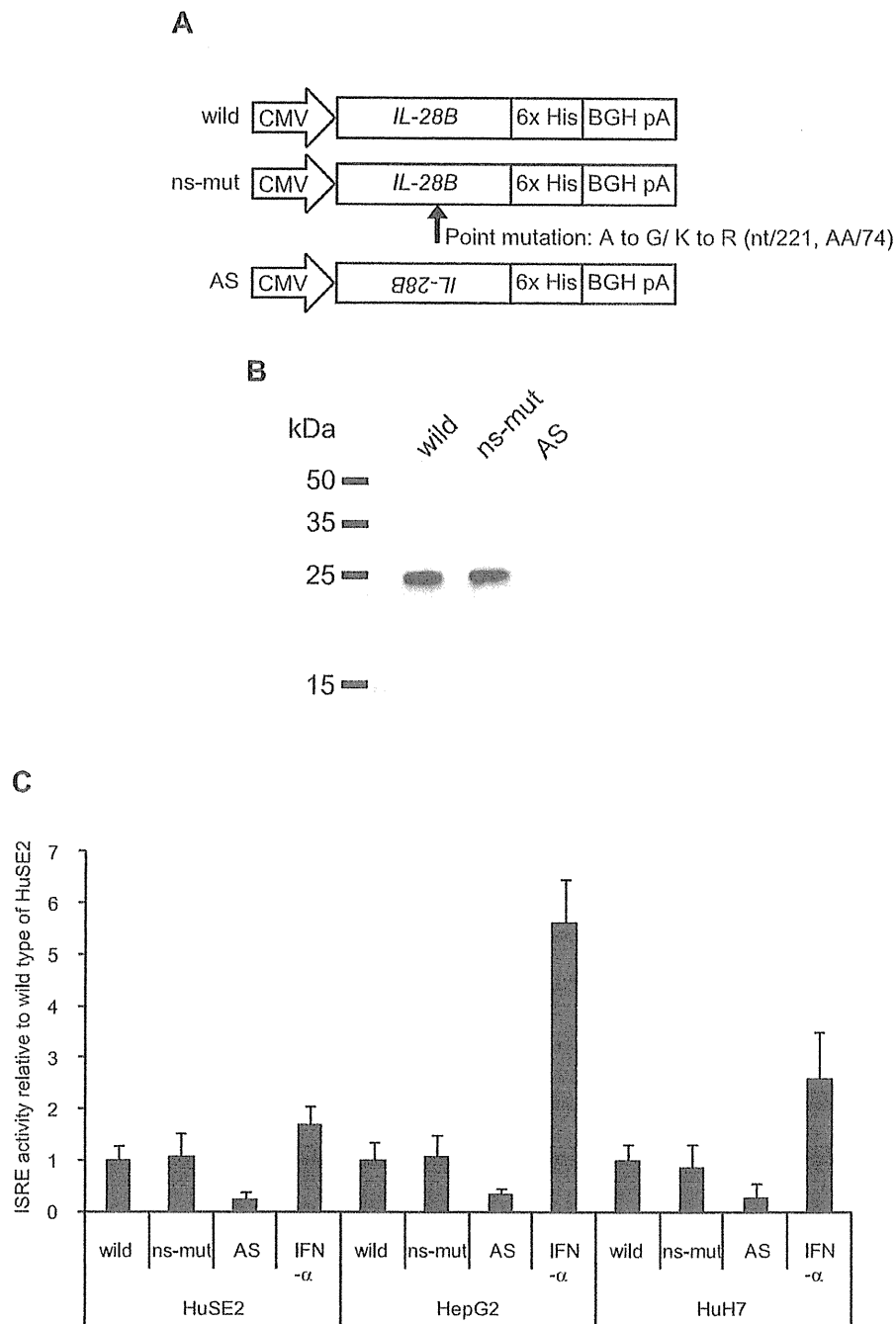doi:10.1371/journal.pone.0026620.g004

- 336 -

A

B

C

Figure 5. The purification and the activity of recombinant IL-28B with or without nsSNP. (A) The 6×His-tagged expression plasmid of wild type, ns-mut, or AS controlled by the CMV promoter was transfected into 293F cells. Schematics are the wild type, ns-mut and AS used in the transfection experiments. The procedure for recombinant protein purification is described in the materials and methods section. (B) The purified products were confirmed by immunoblotting using anti-IL28B antibody and the secondary antibody. The prepared proteins were loaded onto a 12% polyacrylamide gel. Bands corresponding to the expected molecular weight of IL-28B were observed in the wild type and ns-mut lanes. (C) For luciferase assay, HeLa cells were seeded into a 96-well plate at 10^4 cells/well and transfected with pISRE-Luc and pGL4.74 control vector before 16 h of IFN-α or IL-28B stimulation. Five ng/mL of IL-28B wild or ns-mut was added to the culture medium. Flow-though liquid from AS expression was used as a negative control. IFN-α (100 U/mL) was added for positive control of ISRE activity. The luciferase activities were normalized with Renilla activities and data are presented as fold induction from the basal promoter activation of the wild type. Bars indicate the means ± SD of triplicate determinations and the results are from one of three experiments.
doi:10.1371/journal.pone.0026620.g005

Table 2. The variations of TA repeat in *IL-28A* and *28B*.

Gene	Data	Location	
		rs72284792*[1]	rs72258881
IL-28A	RefSeq. (hg19)	(TA)₈	
	Cloning	(TA)₈	
IL-28B	RefSeq. (hg19)		(TA)₁₃
	Cloning		(TA)₁₀₋₁₈

*[1]The ID represents rs72258881, rs59702201, and rs67461793 because these three are located in the same genomic region, the TA repeat.
doi:10.1371/journal.pone.0026620.t002

expression (Fig. 6A). These cells were treated with 100 U/mL of IFN-α and 3 µg/mL of LPS. The results indicated that the variation in the (TA)$_n$ number at this polymorphic locus differentially regulates transcription. The transcriptional activation of the luciferase reporter gene was increased according to the (TA)$_n$ number (Fig. 6B).

Discussion

Four independent GWAS approaches have revealed the significant SNPs associated with response to PEG-IFNα/RBV therapy for CHC [12,13,14,19]. These significant SNPs were

found around *IL-28B* but not *IL-28A*. The SNPs found in clinical studies to determine the outcome of HCV therapy were rs12979860 and rs8099917, because they showed the statistical significance in each study [12,13,14,19]. However, several SNPs around *IL-28B* were in strong LD ($r^2>0.96$) in JPT and CEU populations, although relatively low LD was predicted in the YRI population [16], and so it might be difficult to determine the most informative SNP [16]. These results suggest that any of the SNPs contained in this region could be of predictive value.

As reported in previous studies, transcription of *IL-28A/B* was upregulated in the TT genotype of rs8099917, which was associated with SVR [13,14,20], suggesting that the expression levels of *IL-28B* could be one of the key factors to clear HCV under PEG-IFNα/RBV therapy and could also affect spontaneous clearance of acute HCV infection [15]. To elucidate this question, we examined the function of the SNPs around the *IL-28B* gene to identify those SNPs affecting *IL-28B* expression. The new findings are as follows: 1) the gene structure of *IL-28B* comprised six exons in the several cell lines tested, although it was registered as having five exons in the CCDS database of NCBI. 2) The substitution of intron SNPs and non-synonymous SNPs in the *IL-28B* gene did not influence the expression levels or function. 3) Increased numbers of TA repeats in the promoter region of the *IL-28B* gene enhanced the transcription activity and expression level of the *IL-28B* gene. Because administration of IL-28B has been shown to have antiviral effects [21,22,23], lower expression of IL-28B might lead to a decrease in this effect.
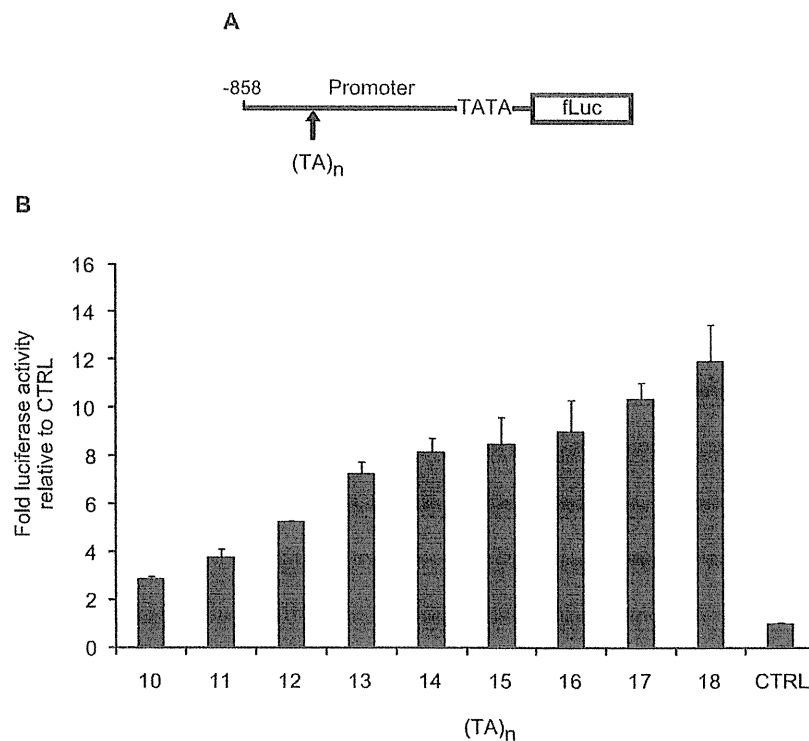
A

B

Figure 6. Luciferase assay of (TA)$_n$ number. (A) *IL-28B* promoter subfragment (nt −858 to +30) modifying (TA)$_n$ number from 10 to 18 was constructed in the pGL4 vector. (B) Raji cells were co-transfected with pGL4 plasmids (0.05 g), and pGL4.74 control plasmid (0.05 g), and tested for firefly as well as renilla luciferase after LPS stimulation (3 µg/mL) for 4 h following IFN-α treatment (100 U/mL) for 16 h. These cells were seeded into a 96-well plate at 10^4 cells/well. The luc activities were normalized with renilla activities and data are presented as fold induction from the activation of the control vector. Bars, the means ± SD of triplicate determinations and the results are from one of three experiments. Statistical analyses are shown in table S4 to avoid complication.
doi:10.1371/journal.pone.0026620.g006

− 338 −

The locations of two SNPs associated with response to HCV therapy, rs8099917 and rs12979860, are approximately 8 kb and 3 kb upstream of *IL-28B* gene, respectively. Because these SNPs, which showed the greatest statistical significance in the previous study, are located far from the *IL-28B* gene, another approach was required to determine the effect of the SNPs. In this study, broad $(TA)_n$ variations were observed in rs8099917 heterozygotes among CHC patients. Interestingly, a combination of TG and 11/12 genotype was strongly associated with NVR, whereas patients harboring the 12/13 genotype showed a virological response, regardless of the TG genotype (rs8099917). In clinical practice, genetic diagnosis using TA variation, following the primary classification of rs8099917 genotype, could improve the prediction of treatment response for CHC patients with the rs8099917 TG genotype. It is not clear whether the variation originates from genetic or epigenetic mechanisms. In addition, as the frequency of TA variation might be dependent on the particular population, further study will be needed to compare the frequency in several populations. A long TA repeat, over $(TA)_{13}$, was observed in healthy volunteers and showed potential for higher gene expression compared with under $(TA)_{13}$ constructs *in vitro*. It may be possible that spontaneous clearance of HCV infection and CHC patients are affected by this region because this also is dependent on *IL-28B* genotype [15,19]. In our speculation, the combination of both TA variation and the landmark SNPs, rs8099917 and rs12979860, might improve the prediction value. In addition, convenient diagnosis method to detect the TA variation like SNPs typing is needed since the present capillary techniques are relative complexity compared with SNPs typing.

In the international database, some SNPs ID are registered in the TA repeat region, located in the regulatory regions of the *IL-28A* and *IL-28B* gene, rs72284792 and rs7225881, respectively, whereas in our analysis separating *IL-28A* from *IL-28*, TA variation was detected only in the *IL-28B* region. SNP data often have been collected using next generation sequencing and based on short sequence reads. Unfortunately, the sequence similarity between *IL-28A* and *IL-28B* is over 90% from the CpG island to the region downstream of 3'-UTR. Alignment failure would occur for a high percentage of sequences when analyzed with software using general algorithms.

Effects of insertion/deletion (indel) polymorphism are known in the field of pharmacogenetic research. A polymorphism in the promoter of the uridine diphosphoglucuronosyl transferase 1A1 (*UGT 1A1*) gene has been shown to cause Crigler-Najjar syndrome types I and II and Gilbert syndrome, a benign form of unconjugated hyperbilirubinemia, and the occurrence of severe toxic events in irinotecan (known as CPT-11) administration [24,25,26]. The polymorphism consists of a $(TA)_n$ repeat in the 5'-promoter region [24,26,27], similar to that in this study. The range of repeat numbers is from $(TA)_5$ to $(TA)_8$ in the *UGT 1A1* gene [28]. The genetic disorder of the TA repeat length affects enzyme activity. The hepatic bilirubin *UGT 1A1* activity of individuals with Gilbert's syndrome is <30% of normal [29]. Irinotecan is used or under evaluation for a broad spectrum of solid tumors. Irinotecan pharmacokinetic parameters display a wide inter-patient variability and are involved in the genesis of toxic side effects [30,31,32,33]. Based on the polymorphism of the TA repeat, previous papers reported the association of irinotecan-induced severe toxicity with Gilbert's syndrome [34,35,36]. The value of genetic diagnosis of the *UGT1A1* polymorphisms prior to irinotecan chemotherapy has been corroborated in a previous study [37]. As similar characteristics were observed in the upstream region of *IL-28B*, the $(TA)_n$ repeat might be associated with disease progression as well as response to anti-HCV treatment.

In terms of epigenetic aspects, the TA variation of *IL-28B* was also suspected to be related to microsatellite instability, because a gap between the significant SNPs and TA variation was observed in this study. DNA mismatch repair (MMR) deficiency causes a high frequency of microsatellite instability (MSI-H), which is characterized by length alterations within simple repeated sequences, microsatellites. Lynch syndrome is primarily due to germline mutations in one of the DNA MMR genes, hMLH1 or hMSH2 [38]. MSI-H is also observed in <15% of colorectal, gastric and endometrial cancers, where it is associated with the hypermethylation of the promoter region of hMLH1 [39,40]. The diagnosis of MSI-H in cancers is therefore useful for identifying patients with Lynch syndrome and the efficacy of chemotherapy [41,42,43,44,45,46].

In conclusion, a (TA) dinucleotide repeat, rs72258881, located in the promoter region, was discovered by our functional studies of the proximal SNPs around *IL-28B*; the transcriptional activity of the promoter increased gradually in a $(TA)_n$ length-dependent manner. Combination diagnosis based on rs8099917 and rs72258881 might provide improved prediction because the $(TA)_n$ variation of *IL-28B* was observed but not that of *IL-28A*. The further study is needed to reveal the association with treatment response using clinical specimens of CHC. These findings suggest that the dinucleotide repeat could be associated with the transcriptional activity of *IL-28B* as well as constituting a predictor to improve prediction of the response to interferon-based HCV treatment.

Supporting Information

Figure S1 Sequence alignment of *IL-28A/B* cDNA retrieved from the database. The cDNA sequences of *IL-28A/B* were retrieved from the international database using accession number. The cDNA data reported by Sheppard et al. are AY129148 (*IL-28A*) and AY129149 (*IL-28B*) indicated with '_S' in the figure, and that of Kotenko et al. are AY184373 (*IL-28A*) and AY184374 (*IL-28B*) indicated with '_K'. Dashed boxes show the start codon predicted by computational analysis of the human genome reported by Sheppard et al. and Kotenko et al. The sequence alignment was calculated with Lasergene software (DNASTAR, Madison, WI).
(PDF)

Figure S2 Structural similarity between *IL-28A* and *IL-28B*. (A) Schematic of *IL-28A/B* gene location (UCSC genome browser). Boxes show the region representing high levels of structural similarity around *IL-28A/B*. (B) Modified schematic of structural similarity with a percentage. (C) Alignment between IL-28A and IL-28B from the CpG island to the region downstream of 3'-UTR. Homologous regions are shown by red characters. High levels of structural similarity were observed in CpG island, regulatory and gene region bypassing the in/del site.
(PDF)

Figure S3 Innate immune receptor expression related to IL-28B regulation. The relevant receptors for this study were confirmed by PCR using specific primers. (A) The mRNA expression of TLR4 was detected in cell lines, HeLa, Jurkat, MT-2, Raji, and PBMC. (B) For the study of cytokine-receptor association, the expression of IL-28RA and IL-10RB second receptor were examined using cDNA obtained from HuH7, HepG2, and HuSE2 cells. Samples without reverse transcriptase were prepared as a negative control in addition to the checking of genome contamination.
(PDF)

Figure S4 Direct sequencing analysis of TA repeat. In the first step to determine $(TA)_n$ genotypes, direct sequencing was

- 339 -

applied to amplicons of *IL-28A* or *28B* separated by gel electrophoresis. Homozygotes of TA repeat showed clear patterns and a high quality value in the bar above, whereas the patterns of heterozygotes were mixed because the length differed between alleles. The mixed patterns are shown in dashed boxes. These mixed products were cloned into the pGEM-Teasy vector to isolate and count the $(TA)_n$ number by sequencing of both alleles. (PDF)

Table S1
(DOC)

Table S2
(DOC)

Table S3
(DOC)

Table S4
(DOC)

Author Contributions

Conceived and designed the experiments: MS YT MN TW MM. Performed the experiments: MS YT. Analyzed the data: MS YT. Contributed reagents/materials/analysis tools: MS YT MN TW MM. Wrote the paper: MS YT MN TW MM.

References

1. Kotenko SV, Gallagher G, Baurin VV, Lewis-Antes A, Shen M, et al. (2003) IFN-lambdas mediate antiviral protection through a distinct class II cytokine receptor complex. Nat Immunol 4: 69–77.
2. Sheppard P, Kindsvogel W, Xu W, Henderson K, Schlutsmeyer S, et al. (2003) IL-28, IL-29 and their class II cytokine receptor IL-28R. Nat Immunol 4: 63–68.
3. Mordstein M, Kochs G, Dumoutier L, Renauld JC, Paludan SR, et al. (2008) Interferon-lambda contributes to innate immunity of mice against influenza A virus but not against hepatotropic viruses. PLoS Pathog 4: e1000151.
4. Sommereyns C, Paul S, Staeheli P, Michiels T (2008) IFN-lambda (IFN-lambda) is expressed in a tissue-dependent fashion and primarily acts on epithelial cells in vivo. PLoS Pathog 4: e1000017.
5. Doyle SE, Schreckhise H, Khuu-Duong K, Henderson K, Rosler R, et al. (2006) Interleukin-29 uses a type 1 interferon-like program to promote antiviral responses in human hepatocytes. Hepatology 44: 896–906.
6. Marcello T, Grakoui A, Barba-Spaeth G, Machlin ES, Kotenko SV, et al. (2006) Interferons alpha and lambda inhibit hepatitis C virus replication with distinct signal transduction and gene regulation kinetics. Gastroenterology 131: 1887–1898.
7. Zhou Z, Hamming OJ, Ank N, Paludan SR, Nielsen AL, et al. (2007) Type III interferon (IFN) induces a type I IFN-like response in a restricted subset of cells through signaling pathways involving both the Jak-STAT pathway and the mitogen-activated protein kinases. J Virol 81: 7749–7758.
8. Bartlett NW, Buttigieg K, Kotenko SV, Smith GL (2005) Murine interferon lambdas (type III interferons) exhibit potent antiviral activity in vivo in a poxvirus infection model. J Gen Virol 86: 1589–1596.
9. Brand S, Zitzmann K, Dambacher J, Beigel F, Olszak T, et al. (2005) SOCS-1 inhibits expression of the antiviral proteins 2′,5′-OAS and MxA induced by the novel interferon-lambdas IL-28A and IL-29. Biochem Biophys Res Commun 331: 543–548.
10. Robek MD, Boyd BS, Chisari FV (2005) Lambda interferon inhibits hepatitis B and C virus replication. J Virol 79: 3851–3854.
11. Zhu H, Butera M, Nelson DR, Liu C (2005) Novel type I interferon IL-28A suppresses hepatitis C viral RNA replication. Virol J 2: 80.
12. Ge D, Fellay J, Thompson AJ, Simon JS, Shianna KV, et al. (2009) Genetic variation in IL28B predicts hepatitis C treatment-induced viral clearance. Nature 461: 399–401.
13. Suppiah V, Moldovan M, Ahlenstiel G, Berg T, Weltman M, et al. (2009) IL28B is associated with response to chronic hepatitis C interferon-alpha and ribavirin therapy. Nat Genet 41: 1100–1104.
14. Tanaka Y, Nishida N, Sugiyama M, Kurosaki M, Matsuura K, et al. (2009) Genome-wide association of IL28B with response to pegylated interferon-alpha and ribavirin therapy for chronic hepatitis C. Nat Genet 41: 1105–1109.
15. Thomas DL, Thio CL, Martin MP, Qi Y, Ge D, et al. (2009) Genetic variation in IL28B and spontaneous clearance of hepatitis C virus. Nature 461: 798–801.
16. Tanaka Y, Nishida N, Sugiyama M, Tokunaga K, Mizokami M (2010) lambda-Interferons and the single nucleotide polymorphisms: A milestone to tailor-made therapy for chronic hepatitis C. Hepatol Res 40: 449–460.
17. Siren J, Pirhonen J, Julkunen I, Matikainen S (2005) IFN-alpha regulates TLR-dependent gene expression of IFN-alpha, IFN-beta, IL-28, and IL-29. J Immunol 174: 1932–1937.
18. Livak KJ, Schmittgen TD (2001) Analysis of relative gene expression data using real-time quantitative PCR and the 2(-Delta Delta C(T)) Method. Methods 25: 402–408.
19. Rauch A, Kutalik Z, Descombes P, Cai T, Di Iulio J, et al. (2010) Genetic variation in IL28B is associated with chronic hepatitis C and treatment failure: a genome-wide association study. Gastroenterology pp 138-1338–1345, 1345 e1331–1337.
20. Fukuhara T, Taketomi A, Motomura T, Okano S, Ninomiya A, et al. (2010) Variants in IL28B in liver recipients and donors correlate with response to peg-interferon and ribavirin therapy for recurrent hepatitis C. Gastroenterology. pp 139-1577–1585, 1585 e1571–1573.
21. Ank N, Iversen MB, Bartholdy C, Staeheli P, Hartmann R, et al. (2008) An important role for type III interferon (IFN-lambda/IL-28) in TLR-induced antiviral activity. J Immunol 180: 2474–2485.
22. Ank N, West H, Bartholdy C, Eriksson K, Thomsen AR, et al. (2006) Lambda interferon (IFN-lambda), a type III IFN, is induced by viruses and IFNs and displays potent antiviral activity against select virus infections in vivo. J Virol 80: 4501–4509.
23. Contoli M, Message SD, Laza-Stanca V, Edwards MR, Wark PA, et al. (2006) Role of deficient type III interferon-lambda production in asthma exacerbations. Nat Med 12: 1023–1026.
24. Bosma PJ, Chowdhury JR, Bakker C, Gantla S, de Boer A, et al. (1995) The genetic basis of the reduced expression of bilirubin UDP-glucuronosyltransferase 1 in Gilbert's syndrome. N Engl J Med 333: 1171–1175.
25. Monaghan G, Ryan M, Seddon R, Hume R, Burchell B (1996) Genetic variation in bilirubin UPD-glucuronosyltransferase gene promoter and Gilbert's syndrome. Lancet 347: 578–581.
26. Raijmakers MT, Jansen PL, Steegers EA, Peters WH (2000) Association of human liver bilirubin UDP-glucuronyltransferase activity with a polymorphism in the promoter region of the UGT1A1 gene. J Hepatol 33: 348–351.
27. Sato H, Adachi Y, Koiwai O (1996) The genetic basis of Gilbert's syndrome. Lancet 347: 557–558.
28. Beutler E, Gelbart T, Demina A (1998) Racial variability in the UDP-glucuronosyltransferase 1 (UGT1A1) promoter: a balanced polymorphism for regulation of bilirubin metabolism? Proc Natl Acad Sci U S A 95: 8170–8174.
29. Yamamoto K, Sato H, Fujiyama Y, Doida Y, Bamba T (1998) Contribution of two missense mutations (G71R and Y486D) of the bilirubin UDP glycosyltransferase (UGT1A1) gene to phenotypes of Gilbert's syndrome and Crigler-Najjar syndrome type II. Biochim Biophys Acta 1406: 267–273.
30. Gupta E, Lestingi TM, Mick R, Ramirez J, Vokes EE, et al. (1994) Metabolic fate of irinotecan in humans: correlation of glucuronidation with diarrhea. Cancer Res 54: 3723–3725.
31. Gupta E, Mick R, Ramirez J, Wang X, Lestingi TM, et al. (1997) Pharmacokinetic and pharmacodynamic evaluation of the topoisomerase inhibitor irinotecan in cancer patients. J Clin Oncol 15: 1502–1510.
32. Rowinsky EK, Grochow LB, Ettinger DS, Sartorius SE, Lubejko BG, et al. (1994) Phase I and pharmacological study of the novel topoisomerase I inhibitor 7-ethyl-10-[4-(1-piperidino)-1-piperidino]carbonyloxycamptothecin (CPT-11) administered as a ninety-minute infusion every 3 weeks. Cancer Res 54: 427–436.
33. Iyer L, King CD, Whitington PF, Green MD, Roy SK, et al. (1998) Genetic predisposition to the metabolism of irinotecan (CPT-11). Role of uridine diphosphate glucuronosyltransferase isoform 1A1 in the glucuronidation of its active metabolite (SN-38) in human liver microsomes. J Clin Invest 101: 847–854.
34. Sugatani J, Yamakawa K, Yoshinari K, Machida T, Takagi H, et al. (2002) Identification of a defect in the UGT1A1 gene promoter and its association with hyperbilirubinemia. Biochem Biophys Res Commun 292: 492–497.
35. Iyanagi T, Emi Y, Ikushiro S (1998) Biochemical and molecular aspects of genetic disorders of bilirubin metabolism. Biochim Biophys Acta 1407: 173–184.
36. Wasserman E, Myara A, Lokiec F, Goldwasser F, Trivin F, et al. (1997) Severe CPT-11 toxicity in patients with Gilbert's syndrome: two case reports. Ann Oncol 8: 1049–1051.
37. Sadee W, Dai Z (2005) Pharmacogenetics/genomics and personalized medicine. Hum Mol Genet 14 Spec No. 2: R207–214.
38. Modrich P (1994) Mismatch repair, genetic stability, and cancer. Science 266: 1959–1960.
39. Lengauer C, Kinzler KW, Vogelstein B (1997) DNA methylation and genetic instability in colorectal cancer cells. Proc Natl Acad Sci U S A 94: 2545–2550.